Lactate production is a prioritized feature of adipocyte metabolism

Received for publication, September 19, 2019, and in revised form, October 31, 2019 Published, Papers in Press, November 5, 2019, DOI 10.1074/jbc.RA119.011178

James R. Krycer[‡§1], Lake-Ee Quek[§¶2], Deanne Francis[‡§3], Daniel J. Fazakerley[‡§‖4], Sarah D. Elkington[‡§], Alexis Diaz-Vegas[‡§], Kristen C. Cooke[‡§], Fiona C. Weiss[‡§], Xiaowen Duan[‡§5], Sergey Kurdyukov[‡§], Ping-Xin Zhou[**‡‡6], Uttam K. Tambar[**7], Akiyoshi Hirayama[§§¶¶8,9], Satsuki Ikeda[§§], Yushi Kamei[§§], Tomoyoshi Soga[§§¶¶9,10], Gregory J. Cooney[§‖‖11,12], and David E. James[‡§‖‖11,13]

*From the [‡]School of Life and Environmental Sciences, [§]Charles Perkins Centre, [‖‖]Sydney Medical School, and [¶]School of Mathematics and Statistics, the University of Sydney, Sydney, New South Wales 2006, Australia, the [‖]Metabolic Research Laboratories, Wellcome Trust-Medical Research Council Institute of Metabolic Science, University of Cambridge, Cambridge CB2 0QQ, United Kingdom, the **Department of Biochemistry, University of Texas Southwestern Medical Center, Dallas, Texas 75390-9038, the [‡‡]School of Basic Medical Sciences, Xinxiang Medical University, Xinxiang, Henan 453003, China, the [§§]Institute for Advanced Biosciences, Keio University, Tsuruoka, Yamagata 997-0052, Japan, and [¶¶]AMED-CREST, Japan Agency for Medical Research and Development (AMED), 1-7-1 Otemachi, Chiyoda-Ku, Tokyo 100-0004, Japan*

Edited by Jeffrey E. Pessin

Adipose tissue is essential for whole-body glucose homeostasis, with a primary role in lipid storage. It has been previously observed that lactate production is also an important metabolic feature of adipocytes, but its relationship to adipose and whole-body glucose disposal remains unclear. Therefore, using a combination of metabolic labeling techniques, here we closely examined lactate production of cultured and primary mammalian adipocytes. Insulin treatment increased glucose uptake and conversion to lactate, with the latter responding more to insulin than did other metabolic fates of glucose. However, lactate production did not just serve as a mechanism to dispose of excess glucose, because we also observed that lactate production in adipocytes did not solely depend on glucose availability and even occurred independently of glucose metabolism. This suggests that lactate production is prioritized in adipocytes. Furthermore, knocking down lactate dehydrogenase specifically in the fat body of *Drosophila* flies lowered circulating lactate and improved whole-body glucose disposal. These results emphasize that lactate production is an additional metabolic role of adipose tissue beyond lipid storage and release.

This work was supported by the Sydney Informatics Hub, funded by the University of Sydney. The authors declare that they have no conflicts of interest with the contents of this article. The contents of the published material are solely the responsibility of the authors and do not reflect the views of the National Health and Medical Research Council. The content is solely the responsibility of the authors and does not necessarily represent the official views of the National Institutes of Health.

This article contains Figs. S1 and S2.

[1] Supported by National Health and Medical Research Council (NHMRC) Early Career Fellowship APP1072440, an Australian Diabetes Society Skip Martin Early-Career Fellowship, a Diabetes Australia Research program grant, and a CPC Early-Career Seed Funding grant.

[2] Supported by the Judith and David Coffey Fund and Cancer Institute NSW Grant CDF181241.

[3] Supported by a CPC Early-Career Seed Funding grant.

[4] Present address: Metabolic Research Laboratories, Wellcome Trust–Medical Research Council Institute of Metabolic Science, University of Cambridge, Cambridge, CB2 0QQ, United Kingdom.

[5] Supported by University of Sydney–China Scholarship Council Postgraduate Research Scholarship 201606270221.

[6] Supported by China Scholarships Council Program Grant 201708410040.

[7] Supported by Welch Foundation Grant I-1748 and National Institutes of Health Grant R01GM102604.

[8] Supported by Japan Society for the Promotion of Science (JSPS) KAKENHI Grants JP18H04804 and JP18K08219 and by Research on Development of New Drugs (GAPFREE) from the Japan Agency for Medical Research and Development (AMED).

[9] Supported by the Yamagata prefectural government and the City of Tsuruoka.

[10] Supported by AMED-CREST from AMED.

[11] Supported by NHMRC Project Grant GNT1086850.

[12] Supported by a Professorial Research Fellowship from the University of Sydney Medical School. To whom correspondence may be addressed: Charles Perkins Centre, the University of Sydney, Sydney, New South Wales 2006, Australia. Tel.: 612-8627-4756; E-mail: gregory.cooney@sydney.edu.au.

[13] Supported by NHMRC Senior Principal Research Fellowship APP1019680 and NHMRC Project Grants GNT1061122 and GNT1086851. To whom correspondence may be addressed: Charles Perkins Centre, the University of Sydney, Sydney, New South Wales 2006, Australia. Tel.: 612-8627-1621; E-mail: david.james@sydney.edu.au.

The importance of adipose tissue in whole-body glucose homeostasis is demonstrated by the detrimental metabolic consequences of lipodystrophies and beneficial effects of thiazolidinedione treatment (1). In fact, reduced adipocyte glucose uptake is one of the earliest defects observed in insulin resistance (2–4). Although the adipose tissue only contributes ~5% to whole-body glucose disposal following a meal in humans (5), experiments in mice have shown that expression of the insulin-responsive glucose transporter, GLUT4, in adipose tissue is essential for whole-body insulin sensitivity (6, 7). Therefore, the way adipocytes metabolize glucose is likely central to whole-body glucose homeostasis.

One of the major functions of adipose tissue is lipid storage (1), with glucose playing a key role as a substrate for lipogenesis and the triglyceride-glycerol backbone. However, we recently performed dynamic tracer metabolomics in cultured adipocytes and found that lactate is a quantitatively substantial fate for glucose.[14] This is counterintuitive for adipocytes because lactate production is typically associated with rapid cellular

[14] L.-E. Quek, J. R. Krycer, S. Ohno, K. Yugi, D. J. Fazakerley, R. Scalzo, S. D. Elkington, Z. Dai, A. Hirayama, S. Ikeda, F. Shoji, K. Suzuki, J. W. Locasale, T. Soga, D. E. James, and S. Kuroda, submitted for publication.

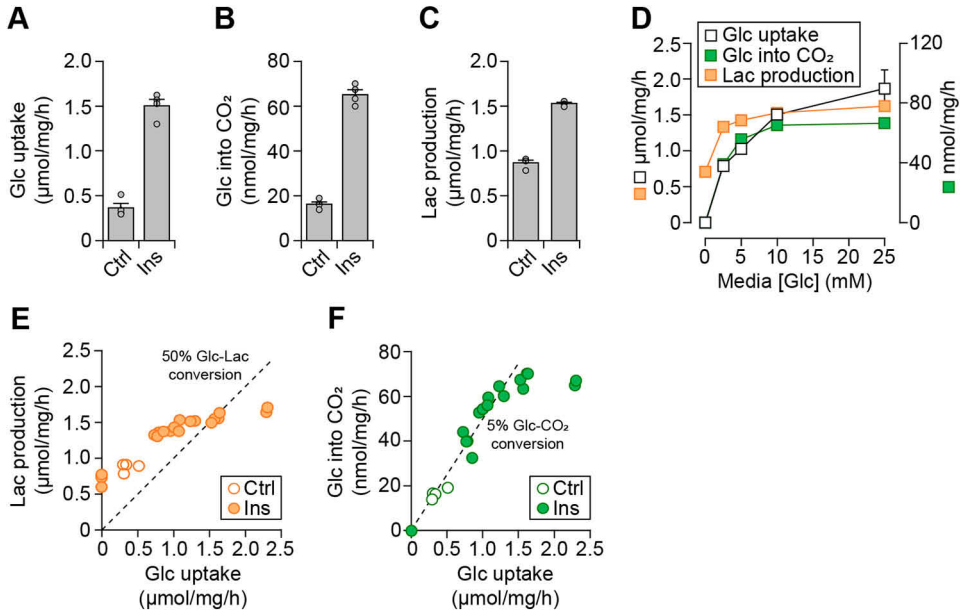

Figure 1. Adipocyte lactate production is not a result of excess glucose availability. *A–C*, 3T3-L1 adipocytes were treated with (*Ins*) or without (*Ctrl*) 100 nM insulin for 1 h in Medium C supplemented with 10 mM glucose (*Glc*). The assay medium also contained [U-^{14}C]Glc tracer for the determination of Glc incorporation into CO_2 (*B*). Following treatment, Glc oxidation (*B*) was determined by gas trapping, and Glc uptake (*A*) and lactate (*Lac*) production (*C*) were determined by enzymatic assays. Data are presented as mean ± S.E. (*error bars*) from four separate experiments. *D*, 3T3-L1 adipocytes were treated with 100 nM Ins for 1 h in Medium C supplemented with varying Glc concentrations. As in *B*, the assay medium also contained [U-^{14}C]Glc tracer for determining Glc oxidation. After the incubation period, Glc uptake, Glc oxidation, and Lac production were determined as in *A–C*. Data are presented as mean ± S.E. (*error bars*) from four separate experiments. Data from *A–D* were derived from the same experiments, with data from the 10 mM Glc + Ins condition replotted between *panels*. *E* and *F*, data from *A–D* replotted, with the inclusion of data from cells treated without insulin in the presence of 10 mM Glc (*Ctrl*). Data presented are from individual experiments.

proliferation (8) or oxygen-limiting conditions, neither of which apply to terminally differentiated adipocytes under normoxia. Nevertheless, this has also been observed in primary adipocytes, characterized in particular by the DiGirolamo laboratory almost 3 decades ago (reviewed in Ref. 9). Intriguingly, they found that lactate production was maintained in insulin-resistant adipocytes, where glucose uptake is reduced (9). This is unusual because lactate production is typically linked to glucose uptake (10). Thus, we sought to clarify the dependence of adipocyte lactate production on glucose availability, using tracer labeling and liquid chromatography-coupled mass spectrometry (LC-MS).[15]

Furthermore, blood lactate is rapidly turned over *in vivo* (11) and can influence glucose homeostasis, with a well-known example being the Cori cycle, where muscle-derived lactate fuels liver glucose production (12). However, to our knowledge, there has been no direct assessment of the role of adipose lactate in whole-body metabolism.

Here, we report that adipose lactate production is not solely linked to glucose availability and is maintained during insulin resistance. Conversely, inhibiting lactate production had little impact on glucose oxidation or glucose uptake in adipocytes. Together, this suggests that adipose lactate production operates independently of glucose uptake. However, on an organismal level, impairing lactate dehydrogenase in the fat body of the *Drosophila* fly markedly improved organismal glucose disposal. Together, this highlights the potential for an underappreciated role for adipocyte glucose metabolism, beyond lipid anabolism, in whole-body glucose homeostasis.

Results

Cultured adipocytes are obliged to produce lactate

In this study, we wished to more closely examine the dependence of adipocyte lactate production on glucose availability. Using cultured adipocytes, insulin treatment markedly increased glucose uptake (Fig. 1*A*), glucose oxidation (Fig. 1*B*), and lactate production (Fig. 1*C*). This concurs with our previous observations that a substantial proportion of glucose is converted to lactate under insulin-stimulated conditions.[14] Thus, we sought to test whether adipocyte lactate production mainly serves to dispose of excess glucose (13), presumably once the flux of glucose to other fates (*e.g.* oxidation to CO_2) becomes fulfilled or saturated. If true, one would expect that significant lactate production would only occur when glucose uptake is high. To test this, we exposed insulin-stimulated adipocytes to a range of glucose concentrations and measured both glucose uptake and lactate production.

Glucose uptake resembled the kinetics of GLUT4, which has a K_m for glucose of 7 mM (14), at which point lactate production was already nearly maximal (Fig. 1*D*). This relationship became more apparent when lactate production was plotted against glucose uptake, which highlighted that substantial lactate production occurred under unstimulated (control) conditions and even when glucose uptake was zero (glucose was not present) (Fig. 1*E*). This was specific to lactate production, because glu-

[15] The abbreviations used are: LC-MS, liquid chromatography-coupled mass spectrometry; DMEM, Dulbecco's modified Eagle's medium; LDH, lactate dehydrogenase; PDH, pyruvate dehydrogenase; Glc, glucose; DCA, dichloroacetate; GNE, GNE-140; TCA, tricarboxylic acid; KD, knockdown; KHB, Krebs–Henseleit buffer.

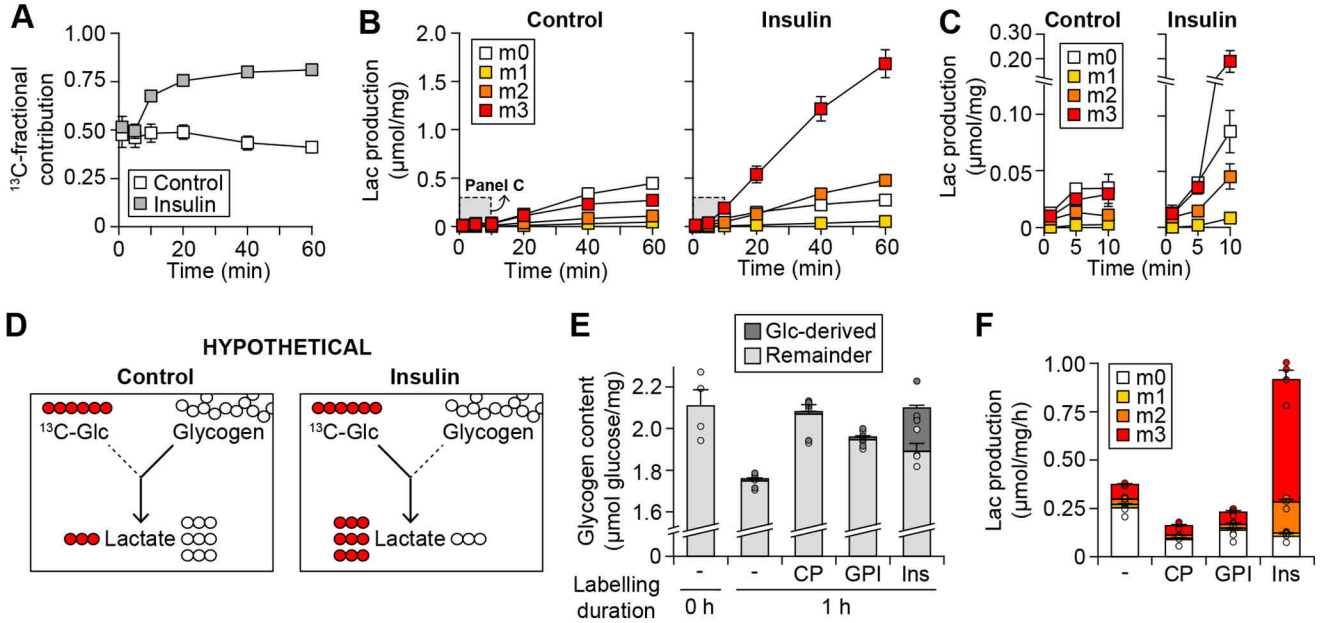

Figure 2. Adipocyte lactate can be derived from nonglucose carbon sources. *A–C*, 3T3-L1 adipocytes were treated with or without 100 nM insulin for 1 h in Medium BS, supplemented with 25 mM [U-^{13}C]glucose. Aliquots of media were taken at the indicated time points and subjected to lactate (*Lac*) determination by LC-MS. Data are depicted as ^{13}C-fractional contribution (*A*) or individual isotopologues (*B* and *C*). Data in *C* are reproduced from *B* to highlight the early time points. Data in *A–C* are presented as mean ± S.D. (*error bars*) from six biological replicates pooled from two separate experiments. The samples from one experiment were generated in a previous study,[14] but were reanalyzed here with our new LC-MS methodology (detailed under "Experimental procedures"). *D*, hypothetical source of lactate carbon for control- or insulin-treated cells. *Red circles*, ^{13}C-labeled carbon atoms. *Glc*, glucose. For details, see "Results." *E*, 3T3-L1 adipocytes were treated for 1 h with or without insulin (*Ins*, 100 nM), CP-91149 (*CP*, 10 μM), or GPI (2 μM), in Medium BS, supplemented with 10 mM glucose and [U-^{14}C]glucose tracer. Cells were harvested either at the start (0 h) or end (1 h) of the treatment period. Glycogen was isolated by Na_2SO_4 precipitation and assessed for glucose incorporation (radioactivity) and total glycogen content. Data are presented as mean ± S.E. (*error bars*) from four separate experiments. *F*, 3T3-L1 adipocytes were treated for 1 h with the same pharmacological agents as in *E*, except in Medium BS supplemented with 25 mM [U-^{13}C]glucose. Following treatment, lactate production was quantified by LC-MS. Data are presented as mean ± S.E. (*error bars*) from four separate experiments.

cose oxidation increased concomitantly with glucose uptake (Fig. 1, *C* and *E*). These relationships were observed when adipocytes were incubated with (Fig. 1) or without (Fig. S1) $NaHCO_3$, which has been found previously to influence cellular respiration (15). Thus, lactate production in adipocytes is not directly related to, and can occur independently of, glucose uptake.

This raises the possibility that at least some of the lactate released from adipocytes is derived from nonglucose sources. To directly quantify the contribution of glucose to lactate output, we cultured adipocytes with ^{13}C-labeled glucose and measured lactate isotopologues using a rapid, targeted LC-MS protocol. Insulin rapidly increased the proportion of lactate derived from exogenous [^{13}C]glucose (^{13}C-fractional contribution) (Fig. 2*A*). Assessing the individual lactate isotopologues, the most abundant isotopologue for insulin-treated adipocytes was the m3 (maximally ^{13}C-enriched) isotopologue (Fig. 2*B*, *right*), where all carbon in lactate originated from the (exogenous) [^{13}C]glucose. This isotopologue became dominant after 10 min of insulin treatment (Fig. 2*C*), matching the kinetics of glucose uptake (16) and glycolytic flux.[14] Together, this demonstrates that lactate was primarily glucose-derived under insulin-stimulated conditions.

However, in the absence of insulin, the unlabeled (m0) isotopologue was dominant (Fig. 2*B*, *left*). We hypothesized that under this condition, lactate was being derived from glycogen breakdown (Fig. 2*D*). Indeed, glycogen content decreased when insulin was absent, whereas insulin maintained cellular glycogen content by utilizing glucose for glycogen synthesis (Fig. 2*E*). Insulin also reduced the amount of m0 lactate produced (Fig. 2*F*). Impairing glycogen breakdown using glycogen phosphorylase inhibitors (Fig. 2*E*) reduced both m0 and total lactate production (Fig. 2*F*). This demonstrated that glycogen can also contribute to lactate production. Overall, lactate production was unlikely to be driven solely by increased glucose availability, but rather a metabolic requirement of adipocytes even when glucose uptake is limiting.

Lactate production occurs in isolated primary adipocytes

To translate these observations from cultured cells to primary adipocytes, rat epididymal adipose tissue was collagenase-digested, and freshly isolated primary adipocytes were subjected to a battery of assays to assess glucose partitioning (Fig. 3*A*). Classically, primary adipocyte metabolism has been studied using buffers where glucose was the only substrate (*e.g.* see Ref. 17). Lactate output was then measured enzymatically and assumed to be solely derived from glucose. Here, we performed our experiments in DMEM, ensuring that other substrates were present, as would be the case for adipocytes *in vivo*, and assessed the incorporation of ^{13}C-labeled glucose into lactate. In parallel, we measured glucose incorporation into CO_2 and lipid.

Glucose conversion into these fates was insulin-responsive (Fig. 3, *B–D*), but lactate was more insulin-responsive than other fates (Fig. 3*E*). To assess how this impacted glucose partitioning, we considered glucose conversion into each fate (lactate, CO_2, and lipid) as a proportion of total glucose metabolism (Fig. 3*F*). Total glucose metabolism was calculated as the sum of

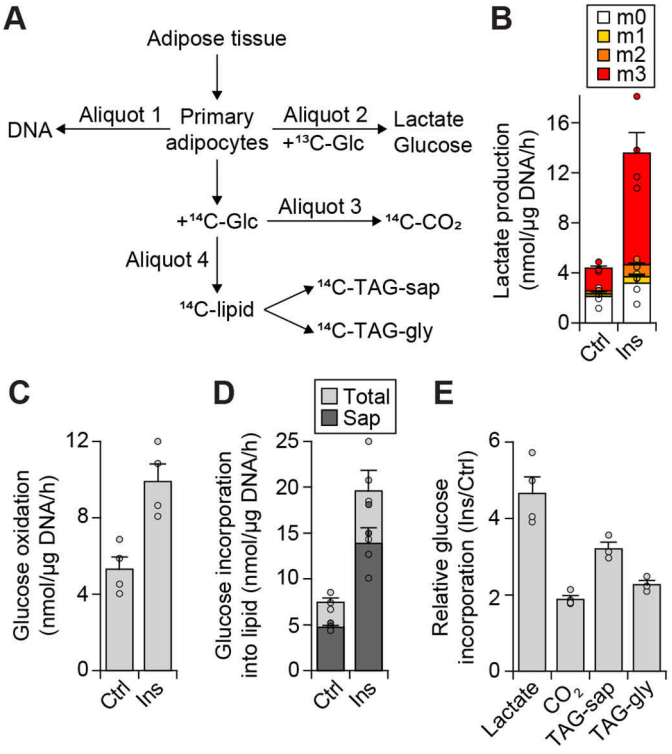

F

		Glc metabolism		Glc uptake
		Ctrl	Ins	Ins
% Glc into	CO_2	40.1 ± 1.3	28.9 ± 1.2	20.7 ± 0.8
	Lactate	7.3 ± 0.6	14.2 ± 1.9	10.1 ± 1.2
	TAG-sap	33.3 ± 1.4	40.2 ± 1.5	29.1 ± 2.8
	TAG-gly	19.3 ± 0.5	16.7 ± 0.8	12.1 ± 1.4
	Unexplained	-	-	28.1 ± 5.1
Total (nmol/µg DNA/h)		14.2 ± 1.3	34.4 ± 3.7	48.1 ± 4.9

Figure 3. Lactate production is a substantial metabolic output of primary adipocytes. *A–D*, mature primary adipocytes were isolated from rats and from each batch, aliquots of adipocytes were subjected to various assays to quantify glucose partitioning (*A*), as detailed under "Experimental procedures." Adipocytes were treated without (control, *Ctrl*) or with insulin (*Ins*, 20 nM) for 1 h. Following treatment, lactate content was determined by LC-MS (*B*), glucose oxidation by gas trapping (*C*), and glucose incorporation into lipid by MeOH-$CHCl_3$ extraction and subsequent saponification (*sap*) (*D*). *E*, ratio between insulin- and control-treated adipocytes, of the amount of glucose carbon incorporated into lactate (*B*), CO_2 (*C*), and lipid (*D*). Lipid data are presented as saponifiable lipid (triacylglyceride (*TAG*)-*sap*) or TAG-glyceride (*TAG-gly*), the latter being the difference between total and saponifiable lipid. *F*, data from *B–D* normalized to total glucose metabolism (sum of glucose incorporated into lactate (*B*), CO_2 (*C*), and lipid fractions (data from *D*, calculated as in *E*) or normalized to glucose uptake, determined by measuring changes in glucose content by enzymatic assay. Data in *B–F* are presented as mean ± S.E. (*error bars*) from four separate batches of isolated adipocytes (except lipid data from control-treated adipocytes, which was $n = 3$).

these fates (as used classically (*e.g.* see Ref. 17)), which could explain a majority (~72%) of the glucose uptake in insulin-treated cells (Fig. 3*F*). This demonstrated that CO_2 and saponified lipid were the major fates of glucose in primary adipocytes (Fig. 3*F*), with similar partitioning observed in previous studies where glucose was the only substrate (17). Only the proportion of glucose incorporated into lactate increased substantially upon insulin stimulation (Fig. 3, *E* and *F*). Indeed, the m3 lactate isotopologue was dominant under insulin-stimulated conditions (Fig. 3*B*). Importantly, the m0 lactate isotopologue was substantial when insulin was absent, accounting for ~47% of total lactate production (Fig. 3*B*), concurring with what we observed in cultured adipocytes (Fig. 2, *A* and *F*). Together, this suggests that lactate production occurs both with and independently of exogenous glucose, similarly to cultured adipocytes.

Lactate production is maintained by adipocytes in insulin resistance

We next examined whether lactate production occurred under insulin-resistant conditions, where insulin-responsive glucose uptake is lowered. In light of our data on lactate production in response to different medium glucose concentrations (Fig. 1), we hypothesized that insulin-resistant adipocytes would maintain lactate production, whether from glucose or other carbon sources. We examined glucose uptake and lactate production in several adipocyte models of insulin resistance (18, 19). This included cultured adipocytes treated with different insults reported to induce insulin resistance *in vivo*. These treatments were chronic exposure to insulin (*CI* in Fig. 4) to mimic hyperinsulinemia, tumor necrosis factor α (*TNF*) to mimic inflammation, and dexamethasone (*Dex*) to mimic anti-inflammatory steroids. Each model exhibited lowered glucose uptake (Fig. 4*A*). In contrast, changes in lactate production were smaller (and mostly not significant) by comparison (Fig. 4*B*). Under insulin-stimulated conditions, the ratio of glucose incorporated into lactate (Fig. 4*C*) (or total lactate output; data not shown) to glucose uptake was higher in the insulin resistance models. Together, this suggests that glucose conversion into lactate is maintained by adipocytes under insulin resistance despite lower glucose uptake.

Glucose oxidation cannot compensate for impaired lactate production

Thus far, our data suggest that lactate production in adipocytes can occur independently of glucose availability, perhaps being prioritized over other end points of glucose metabolism. We hypothesized that if lactate production was impaired, the adipocyte would compensate by diverting glucose to other fates (*e.g.* glucose oxidation). We tested this by diverting glucose flow into the TCA cycle and measured lactate production and glucose oxidation. We chose a pharmacological approach to ensure acute inhibition (<1 h) without long-term adaptive responses. We targeted two key control points, lactate dehydrogenase (LDH) and pyruvate dehydrogenase (PDH), with a panel of inhibitors (Fig. 5*A*). Hypothetically, these inhibitors should reduce lactate production and increase glucose oxidation.

Initially, we used an activator of PDH, dichloroacetate (DCA), which inhibits PDH kinase to derepress PDH activity (Fig. 5*A*). Co-treatment with DCA reduced PDH phosphorylation without affecting total PDH levels (Fig. 5, *B* and *C*), increased glucose oxidation (Fig. S2*A*), and reduced lactate production (Fig. S2*B*). Parenthetically, we also tested a recently developed PDH kinase inhibitor, PS10 (20), but found that this drug had no effect on glucose oxidation (Fig. S2*A*), lactate production (Fig. S2*B*), or PDH phosphorylation (Fig. S2*C*) in cultured adipocytes. We complemented this approach by targeting LDH isoforms with GNE-140 (GNE), a dual LDHA/B inhibitor (21). Total lactate production was similarly reduced

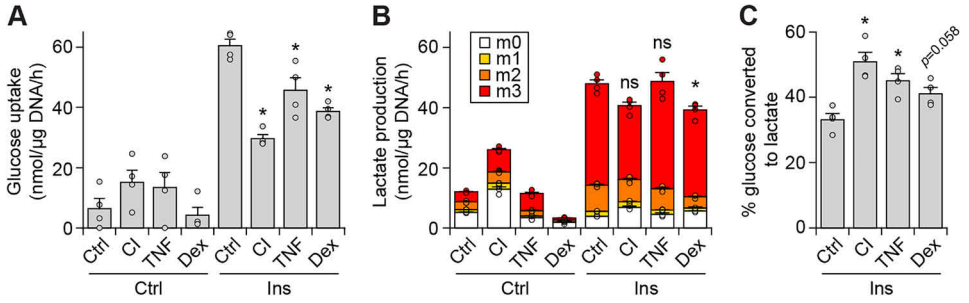

Figure 4. Lactate production is maintained in insulin resistant adipocytes. 3T3-L1 adipocytes were rendered insulin-resistant by either chronic insulin treatment (*CI*), tumor necrosis factor α (*TNF*), or dexamethasone (*Dex*). *A* and *B*, cells were treated for 1 h with or without 100 nM insulin (*Ins*), in Medium C supplemented with 10 mM [U-^{13}C]glucose. Following treatment, glucose uptake (*A*) was determined enzymatically, and lactate production (*B*) was quantified by LC-MS. *C*, the amount of glucose converted to lactate was derived from the amount of ^{13}C-labeled lactate produced (*B*) and presented as a proportion of glucose uptake (*A*). Data in *A–C* are presented as mean ± S.E. (*error bars*) from four separate experiments. *, $p < 0.05$; *ns*, $p > 0.05$, by two-sample *t* test. *Ctrl*, control.

between cells treated with either DCA or GNE (Fig. 5*D*). Interestingly, the distribution of lactate isotopologues varied between the cells treated with each inhibitor (Fig. 5*D*), confirming that they impair lactate production via different mechanisms of action.

Next, we considered glucose oxidation and uptake. GNE also caused a slight increase in glucose oxidation (10.4 ± 1.7% with 25 μM GNE) but had less of an effect than DCA (19 ± 3.9%) (Fig. 5*E*). Nevertheless, neither GNE nor DCA increased glucose oxidation to the same magnitude to which lactate production was decreased (nmol/mg/h scale (Fig. 5*E*) *versus* μmol/mg/h scale (Fig. 5*D*), respectively). Furthermore, glucose uptake was largely unaffected by these inhibitors (Fig. 5*F*), suggesting that upon impaired lactate production, adipocytes did not rely upon glucose oxidation as a major fate to maintain glucose disposal.

We explored this regulation of glucose oxidation further, by comparing glucose metabolism under insulin-stimulated conditions and when bioenergetic demand is maximized with a mitochondrial uncoupler (BAM15). Treatment with BAM15 substantially increased both lactate production (Fig. 5*G*) and glucose oxidation (Fig. 5*H*), even in the presence of DCA or the absence of insulin. Interestingly, glucose uptake did not change with BAM15 treatment (Fig. 5*I*), suggesting that in response to BAM15, adipocytes divert glucose from other metabolic end points to fuel lactate production and glucose oxidation. Overall, this confirmed that adipocytes could increase glucose oxidation under certain circumstances, but this is not observed with impaired lactate production.

Overall, disrupting lactate production did not result in substantial compensation in glucose oxidation or uptake by adipocytes. This suggests a specific role for adipocyte lactate production beyond simply a mechanism for disposing of excess glucose.

Impairing lactate production caused widespread changes in adipocyte metabolism

Consequently, we evaluated how central carbon metabolism, beyond glucose oxidation, responded to impaired lactate production. Consistent with lactate production (Fig. 5*D*), intracellular lactate was lower in response to both DCA and GNE (Fig. 6*A*). We examined the response of other metabolites by considering not only absolute abundance (Fig. 6*A*), but also the ratio of inhibitor- *versus* control-treated cells (Fig. 6*B*). The latter analysis identified "crossover points", whereby adjacent metabolites responded in opposite directions, corresponding to potential sites of regulation (22, 23). For instance, DCA-treated cells exhibited a crossover point between pyruvate and acetyl-CoA (Fig. 6*B*), with less pyruvate (Fig. 6*A*) and increased glucose-derived (^{13}C-labeled) acetyl-CoA (Fig. 6*A*). These data are consistent with DCA-mediated activation of PDH. In contrast, GNE caused a crossover point between pyruvate and lactate (Fig. 6*B*), with more pyruvate (Fig. 6*A*) as expected with LDH inhibition. Together, these data confirmed that these inhibitors impacted lactate production through different mechanisms.

Both inhibitors increased TCA cycle metabolites (Fig. 6, *A* and *B*), except DCA lowered fumarate and malate abundance, likely due to a reduction in pyruvate anaplerosis upon PDH activation. Crossover points were also observed in nucleotide synthesis, between PRPP and other pentose phosphate pathway metabolites, and glycogen synthesis (Fig. 6*B*). Strikingly, there was a crossover point between upper and lower glycolysis with both inhibitors (Fig. 6*B*). This resulted in an accumulation of metabolites in upper glycolysis and glycerol 3-phosphate (Fig. 6*A*). Given the high abundance of glycerol 3-phosphate (Fig. 6*A*), this could act as a potential carbon sink upon inhibition of lactate production. In general, these responses of total metabolite concentrations mirrored those of ^{13}C-labeled metabolites (Fig. 6*B*), suggesting that inhibiting lactate production does not result in the selective usage of glucose over other substrates (or vice versa) for the production of these metabolites.

We also examined cellular energy and redox status (Fig. 6*C–D*). The proportion of NADH (relative to the sum of NADH and NAD^+) increased 3.1-fold with DCA and 1.9-fold with GNE (Fig. 6*D*), consistent with the role of lactate production in maintaining cytosolic redox status. Despite this, the energy charge ratio did not decrease (Fig. 6*C*), suggesting that this did not impact energy production (relative to cellular demands). Overall, this reveals that impairing lactate production causes metabolic changes beyond glucose oxidation in adipocytes.

Lactate production may be important for whole-body glucose disposal

It has been recently reported that there is high lactate turnover at the whole-body level in mice, with lactate serving as a favored substrate for energy production (11). We hypothesized

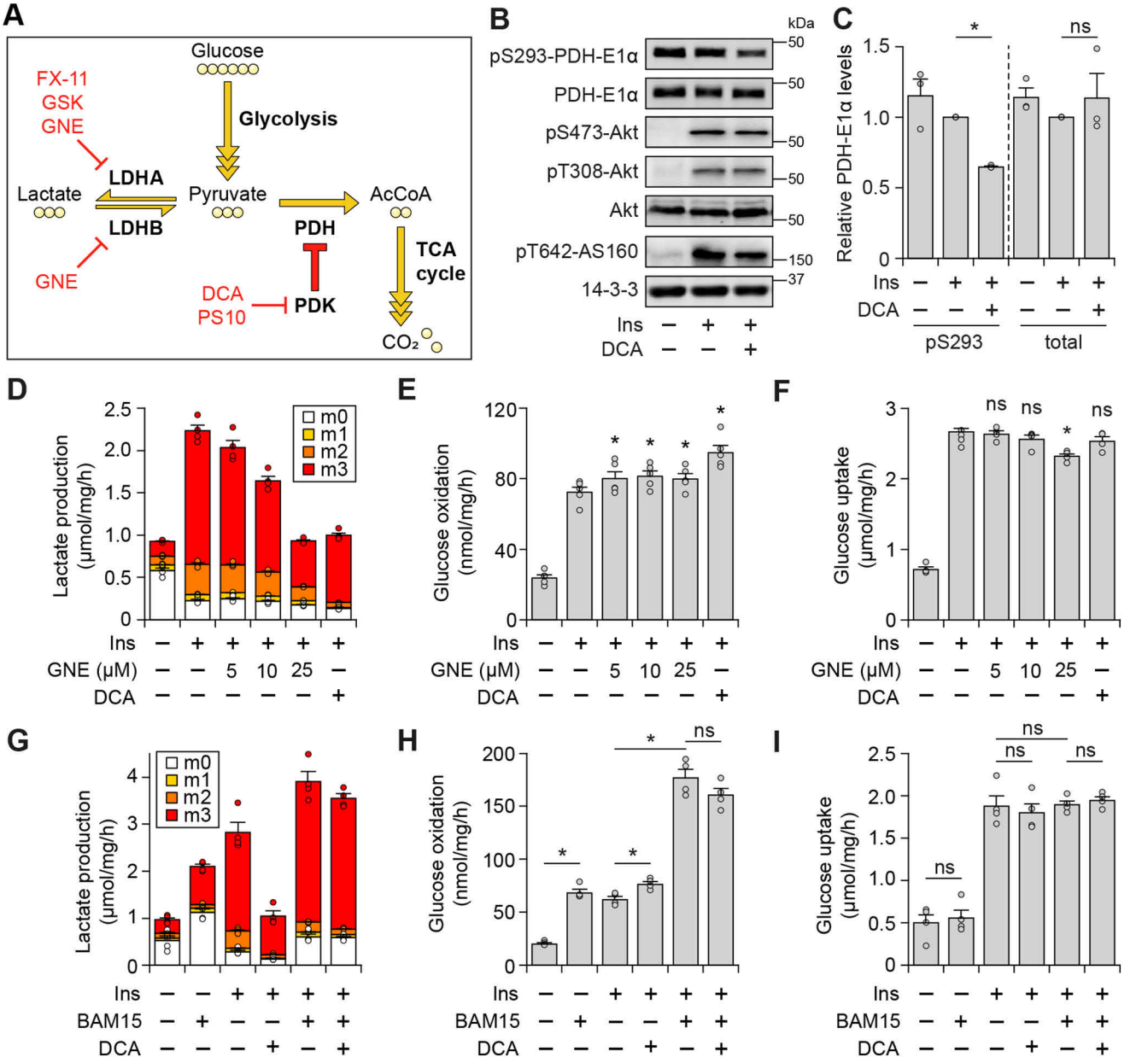

Figure 5. Glucose oxidation cannot compensate for impaired lactate production in adipocytes. *A*, *schematic* depicting the control points in glucose metabolism targeted pharmacologically in this study. *AcCoA*, acetyl-CoA; *GSK*, GSK-2837808A; *PDK*, PDH kinase. *B*, 3T3-L1 adipocytes were treated with or without 1 mM DCA and 100 nM insulin (*Ins*) for 1 h in Medium C, supplemented with 10 mM glucose. Cells receiving DCA were also pretreated with DCA during the last 1 h of the serum starvation period. Following treatment, cells were harvested and lysates were subjected to Western blotting. *C*, quantification of the phosphorylation (pS293) and total levels of PDH-E1α from *B*, normalized to 14-3-3 and made relative to the insulin-only condition. *, $p < 0.05$; *ns*, $p > 0.05$, by two-sample *t* test. *D–F*, 3T3-L1 adipocytes were co-treated with or without 100 nM insulin, 1 mM DCA (without pretreatment), or GNE (at the concentrations indicated) for 1 h in Medium C, supplemented with either 10 mM [U-^{13}C]glucose (*D* and *F*) or 10 mM glucose with [U-^{14}C]glucose tracer (*E*). Cells were assayed for glucose oxidation by gas trapping (*E*), and medium was used to quantify lactate production by LC-MS (*D*) or glucose uptake enzymatically (*F*). Data are presented as mean ± S.E. (*error bars*) from 4–5 separate experiments. In *E* and *F*, *, $p < 0.05$; ns, $p > 0.05$, compared with the insulin-only condition, by two-sample *t* test. *G–I*, 3T3-L1 adipocytes were treated and assayed as in *D–F*, except treatments included 1 mM DCA, 100 nM insulin, and 10 μM BAM15. Data are presented as mean ± S.E. from four separate experiments. In *H* and *I*, *, $p < 0.05$; *ns*, $p > 0.05$, by two-sample *t* test.

that adipose lactate production contributed to whole-body lactate levels. To our knowledge, there is no adipose-specific, LDH-knockout rodent model available. This is further complicated by the presence of two LDH isoforms. Although the pyruvate-to-lactate reaction is considered to be catalyzed mainly by the LDHA isoform, inhibition of LDHA with either GSK-2837808A (24) or FX-11 (25) was insufficient to alter glucose oxidation or lactate production in cultured adipocytes (Fig. S2, *D* and *E*). This suggests that an adipose-specific double LDH knockout would be required to influence adipose metabolism in mammals.

As a proof-of-principle experiment, we utilized *Drosophila*, which only possess one LDH isoform, to examine the effect of restricting lactate production on organismal glucose homeostasis. We knocked down *LDH* (Fig. 7*A*) specifically in the fly fat body. Although the fat body functions as both the adipose and liver tissue in *Drosophila*, seeing any metabolic differences in this model would lend support to the view that adipocyte lac-

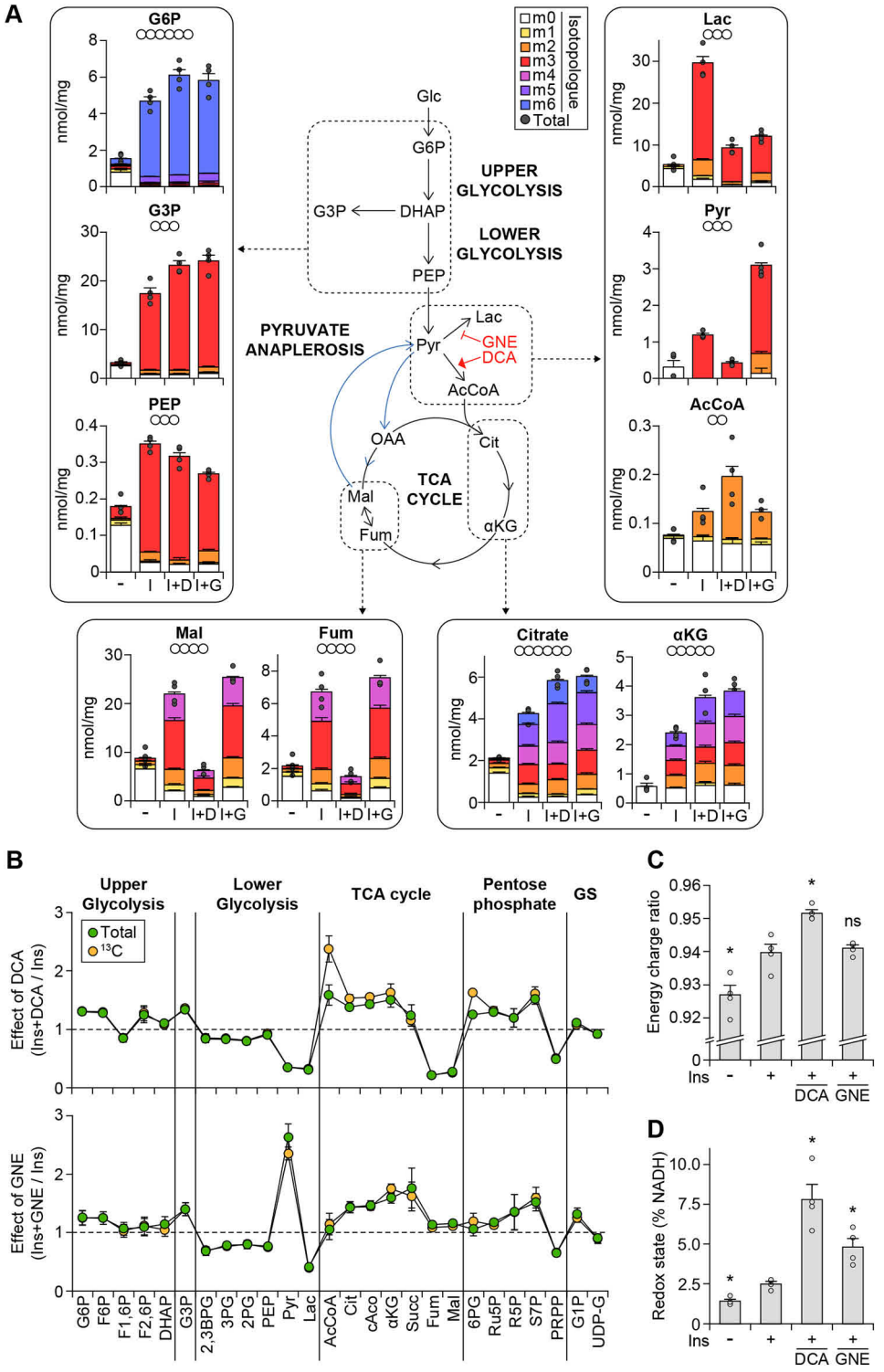

Figure 6. Impairing lactate production causes widespread changes in adipocyte metabolism. *A–D*, 3T3-L1 adipocytes were incubated for 1 h in Medium C, supplemented with 10 mM [U-^{13}C]glucose, in the presence of insulin (*Ins*, 100 nM), DCA (1 mM), and/or GNE (25 μM). Following treatment, intracellular metabolites were extracted and subjected to targeted metabolomics analysis. Data were obtained from four separate experiments. *A*, isotopologue levels for selected metabolites, in the absence (−) or presence of insulin (*I*), insulin and DCA (*I*+*D*), or insulin and GNE (*I*+*G*). The *circles below* each metabolite name denote the number of labeled carbons considered for that metabolite. Data are presented as mean ± S.E. (*error bars*) for individual isotopologues and separate data points for total levels. *B*, effect of DCA and GNE on the total and ^{13}C-labeled metabolite abundance was expressed relative to the insulin-only condition. Data are presented as mean ± S.E. *C*, energy charge ratio was calculated by (ATP + 0.5 ADP)/(ATP + ADP + AMP). Data are presented as mean ± S.E. *D*, redox state was assessed by NADH/(NADH + NAD$^+$), expressed as a percentage. Data are presented as mean ± S.E. For *C* and *D*, *, $p < 0.05$; *ns*, $p > 0.05$, compared with the insulin-only condition, by two-sample *t* test. *2,3BPG*, 2,3-bisphosphoglycerate; *2PG*, 2-phosphoglycerate; *3PG*, 3-phosphoglycerate; *6PG*, 6-phosphogluconate; *AcCoA*, acetyl-CoA; *cAco*, *cis*-aconitate; *Cit*, citrate; *DHAP*, dihydroxyacetone phosphate; *F1,6BP*, fructose 1,6-bisphosphate; *F2,6BP*, fructose 2,6-bisphosphate; *F6P*, fructose 6-phosphate; *Fum*, fumarate; *G1P*, glucose 1-phosphate; *G3P*, glycerol 3-phosphate; *G6P*, glucose 6-phosphate; *GS*, glycogen synthesis; *Lac*, lactate; *Mal*, malate; *PEP*, phosphoenolpyruvate; *PRPP*, phosphoribosyl pyrophosphate; *Pyr*, pyruvate; *R5P*, ribose 5-phosphate; *Ru5P*, ribulose 5-phosphate; *S7P*, sedoheptulose 7-phosphate; *Succ*, succinate; *UDP-G*, uridine diphosphate glucose; *αKG*, α-ketoglutarate.

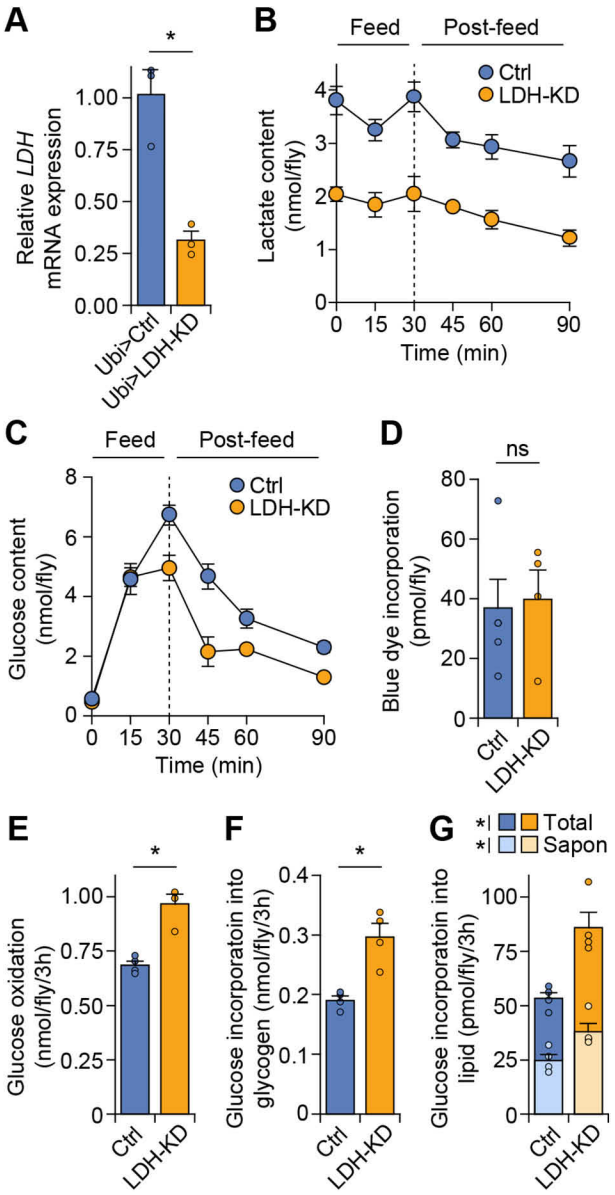

Figure 7. Fat body–specific knockdown of LDH improves whole-body glucose disposal in *Drosophila*. *A*, *Drosophila* flies expressing either whole-body control (*ubi*-GAL4>UAS-CGnone^{GD3003}, Ubi>Ctrl) or LDH-specific (*ubi*-GAL4>UAS-*ldh*^{GD6887}, Ubi>LDH-KD) knockdown were harvested for RNA, and *LDH* RNA expression levels were quantified. Data are presented as mean ± S.E. (*error bars*) from three separate biological replicates. *, $p < 0.05$ by two-sample *t* test. *B* and *C*, *Drosophila* flies expressing fat body–specific control (*cg*-GAL4>UAS-CGnone^{GD3003}, Ctrl) or LDH-specific (*cg*-GAL4>UAS-CGnone^{GD3003}, LDH-KD) knockdown were fasted overnight and subjected to a glucose tolerance test (*GTT*). At specified time points, flies were subjected to MeOH/$CHCl_3$ extraction, after which lactate (*B*) and glucose (*C*) content were determined enzymatically. Data are presented as mean ± S.E., from six separate biological replicates for each time point from a single GTT experiment, representative of three separate GTT experiments. *D*, *Drosophila* flies expressing fat body–specific Ctrl or LDH-KD were fasted overnight and subjected to the 30-min "feed" phase of the GTT, in the presence of blue dye. Blue dye was then extracted and quantified by spectrophotometry. Data are presented as mean ± S.E. from 4–5 separate biological replicates from a single experiment, representative of three separate experiments. *ns*, $p > 0.05$ by two-sample *t* test. *E–G*, *Drosophila* flies expressing fat body–specific Ctrl or LDH-KD were fasted overnight and incubated for 3 h in gas traps with food containing [U-^{14}C]glucose. At the end of the incubation period, glucose oxidation was determined using the gas-trapping solution (*E*), whereas flies were subjected to Na_2SO_4 precipitation for glycogen (*F*) or MeOH-$CHCl_3$ extraction and saponification for lipid (*G*). In *G*, glucose incorporation into both total and saponifiable (*sapon*) lipid fractions is presented. Data in *E–G* are presented as mean ± S.E., from four separate biological replicates. *, $p < 0.05$ by two-sample *t* test.

tate metabolism plays an important role in whole-body metabolism.

To examine the impact of fat body–specific LDH knockdown (LDH-KD) on total lactate levels, we challenged flies with a glucose tolerance test. This involved fasting flies overnight and feeding them a high-glucose solution for 30 min before assessing whole-fly glucose content at specified times during another fasting period. We found that fat body–specific LDH-KD reduced total fly lactate at every time point (Fig. 7*B*).

We speculated that this would lead to enhanced utilization of alternate substrates, such as glucose. Indeed, we found that fat body–specific LDH-KD improved glucose tolerance (Fig. 7*C*). Importantly, flies do not synthesize glucose via gluconeogenesis *per se*, instead utilizing trehalose as their dominant circulating sugar (26, 27). Thus, any change in glucose levels reflects the balance between dietary consumption and glucose utilization. Normalizing to the glucose content at 30 min within each strain, we found a lower area under the curve for LDH-KD flies (3,393% × min (control) and 2,812% × min (LDH-KD); Fig. 7*C*), suggesting that LDH-KD increases glucose utilization. Furthermore, LDH-KD had no effect on the incorporation of blue dye during the feeding period (Fig. 7*D*), which can serve as a surrogate for food intake during short-term experiments (28). To specifically assess glucose utilization, we provided flies with a diet containing radiolabeled [U-^{14}C]glucose (29) and found that LDH-KD increased glucose incorporation into CO_2 (Fig. 7*E*), glycogen (Fig. 7*F*), and lipid (Fig. 7*G*). Together, this demonstrates that fat body–specific LDH-KD reduces total fly lactate levels and enhances whole-body glucose utilization in flies.

Discussion

In this study, we closely examined lactate production of cultured and primary adipocytes, particularly its reliance and impact on glucose disposal. As expected, insulin stimulated the incorporation of glucose into lactate, leading to increased lactate production (Figs. 1–3). However, we also found that lactate production can occur independently of glucose availability (Figs. 1–3) and was maintained during insulin resistance (Fig. 4). Conversely, impairing lactate production in adipocytes neither reduced glucose uptake nor was compensated for by increased glucose oxidation (Fig. 5). Nevertheless, targeting fat-body lactate dehydrogenase to reduce lactate production in *Drosophila* improved organismal glucose disposal (Fig. 7). These data highlight lactate production as an important aspect of adipocyte metabolism.

To translate our findings in cultured adipocytes, we examined glucose partitioning in primary adipocytes. Past studies had incubated primary adipocytes in a buffer where glucose was the only substrate and measured lactate enzymatically (*e.g.* see Ref. 17), assuming that exogenous glucose was the dominant substrate for lactate. Here, we utilized ^{13}C-labeling and LC-MS to show that this is the case only under insulin-stimulated conditions. Furthermore, it is well-known that cellular metabolism depends on the buffer system (15, 30). In contrast to previous studies, we used a buffer that also contained vitamins and amino acids (DMEM) and yet found a similar partitioning of glucose (*e.g.* see Ref. 17), demonstrating the robustness of glucose metabolism in adipocytes.

We observed clear differences between cultured and primary adipocytes. In particular, the incorporation of glucose into lactate was higher in cultured adipocytes (~30%) *versus* primary adipocytes (~10%). Although differences could arise from long-term *in vitro* cell culture (and immortalization), another possibility is the impact of cell density. One study demonstrated that increasing the density of primary adipocytes led to a reduction in lactate production and increased glucose incorporation into fatty acids and CO_2 (31). It is possible that as a monolayer, cultured adipocytes reflect a low-density scenario. Nevertheless, in both primary and cultured adipocytes, we found that lactate production has a high degree of insulin-responsiveness compared with glucose oxidation (Fig. 3*F* and Fig. S2*F*) and was glucose-derived under insulin-stimulated conditions (Figs. 2 and 3*B*). Importantly, although lactate production was glucose-responsive, substantial lactate production still occurred from nonglucose sources in primary and cultured adipocytes (Figs. 2 and 3*B*).

Lactate production was also maintained in cultured adipocytes rendered insulin-resistant, despite impaired insulin-responsive glucose uptake. This has also been observed in isolated adipocytes from diabetic human subjects (32), adipose explants from obese human subjects (33), and primary adipocytes derived from rats exposed to long-term fasting (34–36) or a high-fat diet (37), as well as older, obese rats (17, 34, 35, 38). This would suggest that lactate production is prioritized, such that as glucose uptake is lowered, other (lower-priority) fates of glucose are reduced at the expense of maintaining lactate production. Mechanistically, we speculate that this could happen due to a combination of impaired anti-lipolysis and glucose uptake (and fatty acid esterification) leading to an accumulation of free fatty acids, which would suppress oxidation of other substrates and thus divert (glucose) carbon to lactate. Together, this demonstrates that adipose lactate production is maintained even under conditions of reduced glucose uptake.

Collectively, our results suggest that there are two aspects to lactate production in adipocytes. First, insulin stimulates glucose uptake and incorporation into lactate, with lactate production responding more to insulin than other fates of glucose, such as oxidation (Fig. 3*F* and Fig. S2*F*). This is intuitive, as lactate can provide a carbon sink for handling high glucose influx. Furthermore, LDH balances changes in cytosolic redox status arising from glycolysis, concurring with a more reduced environment (more NADH) observed upon the inhibition of lactate production (Fig. 6). Second, lactate production appears to be maintained when glucose uptake is diminished, with alternate carbon sources (*e.g.* glycogen) being relied upon if glucose substrate is insufficient to sustain lactate production. Parenthetically, inhibition of glycogen phosphorylase did not completely abolish unlabeled (nonglucose-derived) lactate (Fig. 2*F*), and we speculate that glucogenic amino acids also contribute to lactate production. Overall, lactate production appears to be prioritized in adipocyte metabolism, independent of glucose availability.

If adipose lactate production does not serve to dispose of excess glucose, what is its physiological role? Studies in mice have shown that lactate has a high turnover rate *in vivo* (11), with most tissues except the brain utilizing lactate. Furthermore, blood lactate rises in humans after a meal or a glucose load (9) but is constitutively higher (with a diminished response) in obese and/or insulin-resistant individuals (9, 39, 40). However, it is currently unclear which tissues are high lactate producers. It has been observed that the up-regulation of key glycolytic enzymes predisposes cells to lactate production, suggesting that this is a common feature during carcinogenesis, immune cell activation, and angiogenesis (10). Among differentiated cells, astrocytes are well-known producers of lactate, with astrocyte cultures producing lactate at a similar magnitude (nmol of lactate released/mg of protein) to cultured adipocytes in this study (*e.g.* see Refs. 41 and 42) and glycogen stores fueling lactate production (42). Furthermore, studies in perfused heart muscle have found lactate to be a significant output for glucose under resting conditions (*e.g.* see Ref. 43). However, there is mixed evidence about the contribution of muscle to lactate output in the resting or postabsorptive state in humans (44–47). Nevertheless, adipose tissue has been consistently shown to be a contributor to blood lactate in both the fasting and postabsorptive state in human subjects (45, 46, 48–51). Furthermore, although oxygen delivery to adipose tissue is diminished with obesity in humans, oxygen availability appeared adequate for adipose metabolism, consuming substantially less oxygen than skeletal muscle (49). This suggests that the obligatory production of lactate could be to generate cytosolic ATP in a tissue that has a low ability to oxidatively generate ATP. Together, these studies suggest that adipose lactate production may contribute substantially to whole-body lactate turnover, but because they primarily relied on arteriovenous differences, the quantitative contribution of adipose tissue (and other tissues) to whole-body lactate turnover remains to be determined.

To our knowledge, there are no rodent models where LDH isoforms have been knocked out in metabolic tissues. One significant challenge would be the redundancy between LDH isoforms; in our hands, a dual-LDH inhibitor was required to reduce lactate production in cultured adipocytes (Fig. 5 and Fig. S2). Thus, we tested the metabolic impact of reducing lactate production using *Drosophila*, which only possess one LDH isoform. Fat body–specific LDH-KD dramatically reduced total fly lactate levels. Although a caveat to these experiments is that the fat body functions as a combination of liver and adipose tissue in flies, these results provide evidence of the potential quantitative significance of adipose lactate production to whole-body lactate turnover.

Interestingly, we found that reducing lactate production by targeting either LDH or PDH did not substantially affect adipocyte glucose uptake or oxidation, compared with the decrease in lactate production. This implies that glucose is diverted to other fates under these conditions. For instance, we observed a disconnect between upper and lower glycolysis, concurring with GAPDH being a flux-controlling step in adipocyte metabolism.[14] This enabled glycerol 3-phosphate to act as a carbon sink when lactate production was impaired. Furthermore, altered cellular redox would alter metabolic flux (*e.g.* the inhibition of GAPDH by a high $NADH/NAD^+$ ratio may contribute to the disconnect in glycolysis) (Fig. 6). The repartitioning of glucose carbon remains the subject of further investigation. Nevertheless, this provides further evidence that lactate

production can vary independently of adipocyte glucose uptake. Despite this, fat body–specific LDH-KD led to a substantial improvement in whole-body glucose disposal. This suggests that lactate production, at least in flies, significantly impacts glucose utilization by other tissues and thus whole-body glucose homeostasis. It has been demonstrated in isolated rat soleus muscle that lactate can suppress glucose oxidation (52), and lactate itself can act as a substrate for synthesizing glucose and glycogen (12, 53). This implies that adipocyte lactate production, and a high lactate turnover in general, may "spare" glucose utilization *in vivo*. Given recent evidence that lactate itself may act as a signaling molecule (54), there are several avenues by which lactate production from adipose tissue may influence whole-body glucose homeostasis and could contribute an additional mechanism for impaired glucose disposal in obese individuals.

Overall, these data highlight lactate production as an additional metabolic role of adipose tissue, not solely dependent on glucose availability and with the potential to have a significant impact on mammalian glucose homeostasis. It would be of great interest to see whether this metabolic feature is shared by other metabolic tissues and whether this can be targeted therapeutically as a means of improving glucose disposal in the treatment of metabolic disease.

Experimental procedures

Pharmacological agents

The following chemicals were used in this study: insulin (Sigma-Aldrich #I5500), CP-91149 (Selleck Chemicals #S2717), GPI (Cayman #17578), FX-11 (Calbiochem, Merck-Millipore #427218), GSK-2837808A (Tocris #5189), GNE-140 ((*R*)-stereoisomer, MedChemExpress #HY-100742A/CS-7646), and dichloroacetate (sodium salt; Sigma-Aldrich #347795). In addition, BAM15 was a gift from Dr. Kyle Hoehn (University of New South Wales, Sydney, Australia), and PS10 was prepared as described previously (20).

Cell culture

3T3-L1 fibroblasts were maintained as described previously (55). Briefly, cells were cultured at 37 °C with 10% CO_2 in Medium A, consisting of bicarbonate-buffered DMEM (Life Technologies, Inc., #11960), supplemented with 10% (v/v) fetal bovine serum (Life Technologies #16000044) and 2 mM GlutaMAX (Life Technologies #35050061). 3T3-L1 fibroblasts were differentiated into adipocytes as described previously (16, 55). Adipocytes were used between days 9–12 after the initiation of differentiation, with the exception of insulin resistance models (see below). At least 90% of the cells were differentiated prior to experiments. These cells were routinely tested for mycoplasma infection.

Insulin resistance models involved 3T3-L1 adipocytes being treated with either chronic insulin, tumor necrosis factor α, or dexamethasone as described previously (18), with experiments being performed on day 13 after the initiation of differentiation.

Unless otherwise specified, prior to insulin stimulation treatments, cells were serum-starved for at least 2 h. This involved being washed three times with PBS and incubated in Medium B, which consisted of bicarbonate-buffered DMEM (Thermo Fisher #11960), supplemented with 0.2% (w/v) BSA (Bovostar) and 2 mM GlutaMAX.

For experiments within the CO_2 incubator, cells were washed twice after the serum starvation period: once with PBS and then with BSF-DMEM, which consisted of substrate-free DMEM (Sigma-Aldrich #D5030), supplemented with 44 mM $NaHCO_3$ and adjusted to pH 7.4 with CO_2 (dry ice). Cells were then incubated in Medium BS, which consisted of BSF-DMEM, supplemented with 0.2% (w/v) BSA, 1 mM GlutaMAX, 1 mM glutamine, and glucose at a concentration specified in the figure legends. Experiments were performed at 37 °C with 10% CO_2.

For metabolic assays outside of the CO_2 incubator (*e.g.* glucose oxidation, where the CO_2-trapping assay is not compatible with a CO_2 incubator), cells were washed twice after the serum starvation period: once with PBS and then with HSF-DMEM, which consisted of substrate-free DMEM (Sigma-Aldrich #D5030) supplemented with 30 mM Na-HEPES (pH 7.4) and adjusted to pH 7.4 with NaOH. Cells were then incubated in Medium C, which consisted of HSF-DMEM, supplemented with 0.2% (w/v) BSA, 1 mM $NaHCO_3$ (added fresh), 1 mM glutamine, 1 mM GlutaMAX, and glucose; unless otherwise specified, Medium C contained 10 mM glucose. Following the addition of assay media and drug treatments, plates were sealed with TopSeal-A PLUS (PerkinElmer Life Sciences) and incubated in a 37 °C incubator.

For ^{13}C-tracer experiments, glucose was replaced with [U-^{13}C]glucose (Omicron Biochemicals #GLC-082). For ^{14}C-radiotracer experiments, the medium was supplemented with 0.5–2 μCi/ml [U-^{14}C]glucose (PerkinElmer Life Sciences #NEC042X001MC) tracer in addition to the 10 mM "cold" glucose.

Measurement of glucose oxidation in cells

The incorporation of [^{14}C]glucose into CO_2 by cells was measured as described previously (56). Briefly, after the addition of assay media and drug treatments, a gas trap containing 2 M NaOH was installed, and plates were sealed with TopSeal-A PLUS (PerkinElmer Life Sciences). Using naive media, we confirmed that the gas trap system did not promote alkalinization of Medium C (data not shown). Following treatment, cells were acidified with perchloric acid, and the radioactivity of the gas-trapping solution was assessed by liquid scintillation counting. Cell-free controls were performed to account for any cell-independent signal.

Measurement of glucose uptake and lactate production by cultured cells

Following treatment, the plate of cells was chilled on ice, and the conditioned medium was removed. Medium was centrifuged for 5 min at 2,000 × *g* to remove debris and measured for glucose (enzymatically) and lactate (enzymatically or by LC-MS) content as described below.

Quantification of lactate by enzymatic assay

Conditioned medium was assayed enzymatically using the hydrazine sink method as described previously (57). Briefly, the assay buffer was 1 M glycine, pH 9.2, 0.4 M hydrazine sulfate in 1 M NaOH, and 2.5 mM EDTA, adjusted to pH 9.2 with NaOH

prior to the addition of 4 mM NAD^+ and 2 units/ml lactate dehydrogenase (Roche Applied Science). An aliquot of medium sample was diluted in water (100 μl total) and incubated with 100 μl of assay buffer in a microplate format. Reactions were protected from light and incubated at room temperature for at least 1 h, after which the absorbance of NADH was measured at 340 nm. Reactions with medium samples without lactate dehydrogenase were included as a negative control. Lactate levels were quantified using a standard curve of lactate, added to naive culture medium.

Quantification of glucose by enzymatic assay

Glucose content was measured with a coupled reaction between glucose oxidase and peroxidase, using an assay kit (Thermo #TR15221). Samples were diluted up to 30 μl with water and incubated with 150 μl of reagent, with the assay otherwise performed according to the manufacturer's instructions. Glucose levels were quantified using a standard curve of glucose, added to the same matrix as the sample except without glucose (*e.g.* added to naive, glucose-free Medium C for experiments where cells were incubated with Medium C). Naive treatment medium was included as a positive control. Glucose uptake was determined by the disappearance of medium glucose, obtained by subtracting the glucose content of the conditioned medium from the naive treatment medium. For this calculation, negative values were adjusted to zero.

Isolation and quantification of glycogen

Glycogen was isolated using the Na_2SO_4 precipitation method, as described previously (16, 58, 59) with some minor modifications. Following treatment (in cell culture plates), cells were washed three times with ice-cold PBS, aspirated dry, and frozen at −20 °C. The plate was thawed on ice, and each well was scraped in 200 μl of 1 M KOH. Samples were incubated in the ThermoMixer C (Eppendorf) for 20 min at 70 °C, with shaking at 1,000 rpm. Following the addition of 75 μl of saturated Na_2SO_4 and 1 ml of ethanol, lysates were vortexed briefly and centrifuged at 16,000 × *g* and 4 °C for 15 min. The pellet was washed by resuspending in 180 μl of water using the ThermoMixer C at 1,000 rpm and 70 °C, adding 1.62 ml of ethanol, and vortexing the mixture briefly before centrifugation at 16,000 × *g* and 4 °C for 15 min. The pellet was dissolved in 400 μl of water using the ThermoMixer C at 1,000 rpm and 70 °C.

The incorporation of (^{14}C-labeled) glucose into glycogen was quantified by measuring radioactivity. Half the sample was mixed with Ultima Gold XR scintillation fluid (PerkinElmer Life Sciences) and subjected to liquid scintillation counting using the Tri-Carb 2810 TR scintillation counter (PerkinElmer Life Sciences). Total glycogen content was determined by incubating the remainder of the sample in 0.25 M sodium acetate (pH 4.75) with 0.3 mg/ml amyloglucosidase (Sigma #A1602) for 4 h at 37 °C with occasional shaking. These samples were then assayed for glucose content, quantified enzymatically as described above.

Quantification of lactate by LC-MS

Metabolites were extracted from conditioned medium as described previously,[14] with minor modifications. Specifically, medium samples were combined with 4 volumes of extraction buffer containing a 1:1 (v/v) mixture of LC-MS grade methanol and acetonitrile (Thermo), with 0.25 μM D-camphor-10-sulfonic acid (Wako #037-01032) internal standard. The mixture was vortexed briefly and centrifuged for 20 min at 16,000 × *g* and 4 °C. The supernatant was lyophilized using an EZ-2 centrifugal evaporator (GeneVac), resuspended in water, recentrifuged, and supernatant was transferred into HPLC vials.

Metabolites were resolved by LC as described previously (60), with several modifications to achieve a rapid, targeted assay for lactate quantification; the total run time was 10 min (*versus* 25 min for the original method). LC separation was achieved using an Infinity 1260 pump (Agilent) with a Synergi Hydro-RP column (Phenomenex, 100-mm length × 2.1-mm internal diameter, 2.5-μm particle size). Buffer A was 95:5 (v/v) water/acetonitrile containing 10 mM tributylamine and 15 mM acetic acid (pH 4.9), and buffer B was 100% acetonitrile. The LC gradient was as follows: 0 min, 10% B, 200 μl/min; 0.5 min, 10% B, 200 μl/min; 1.5 min, 70% B, 200 μl/min; 4 min, 70% B, 200 μl/min; 4.5 min, 10% B, 300 μl/min; 9.5 min, 10% B, 300 μl/min; 10 min, 10% B, 200 μl/min. Autosampler temperature was 4 °C, and column temperature was 25 °C. Injection volume was 5 μl. MS analysis was performed using an AB Sciex QTRAP 5500, with MS source temperature set to 350 °C. Multiple-reaction monitoring transitions were calibrated to include lactate isotopologues (61), and acquisition was performed with a 40-ms dwell time. Calibration standards were diluted in naive medium and then extracted and subjected to LC-MS in parallel to the samples.

LC-MS data were extracted using MSconvert (version 3.0.18165-fd93202f5) and in-house MATLAB scripts. Natural abundance correction was performed as described previously (16). These data were used to calculate the ^{13}C-labeled fractional contribution as described previously (62). The abundance of ^{13}C-labeled lactate was calculated as the product of fractional contribution and total abundance of metabolite (16), representing the amount of fully ^{13}C-labeled lactate. For instance, 1 mol of m1-labeled lactate (lactate with one of its three carbon atoms ^{13}C-labeled) is equivalent to 0.33 mol of fully labeled (m3-labeled) lactate. Furthermore, because one glucose molecule generates two lactate molecules, the ^{13}C-labeled abundance of lactate was then halved to obtain the amount of [^{13}C]glucose incorporated into lactate.

Quantification of intracellular metabolites by targeted metabolomics

Following treatment, cells were washed twice with cold 5% (w/v) mannitol on ice and quenched by freezing the plates on dry ice. Intracellular metabolites were extracted and analyzed by capillary electrophoresis– and ion chromatography–coupled MS as described previously (16), with the exception that fructose bisphosphates were measured using the latter rather than the former metabolomics platform. Data analysis, including natural abundance correction and derivation of ^{13}C-labeled abundance, was performed as described previously (16) and above for lactate quantification.

Normalization for cell culture experiments

Unless otherwise specified, data were normalized to protein content, either from an aliquot of cell lysate used in the respective assay or derived from cells treated in parallel. Protein quantification was performed using the Pierce bicinchoninic acid assay kit (Thermo Fisher Scientific), according to the manufacturer's instructions.

DNA quantification was performed as described previously (63), except adapted for non-96-well culture plates. Following treatment, cells were washed three times with ice-cold PBS, aspirated dry, and frozen. The plate was then thawed at room temperature, and water was added to each well (*e.g.* 500 μl per well for a 12-well plate). After at least three freeze-thaw cycles were performed, 1 volume of TNE buffer (10 mM Tris-HCl, pH 7.4, 2 M NaCl, 1 mM EDTA) was added to each well, cells were scraped, and lysates were gently mixed within each well by pipetting. Aliquots of lysate were transferred to a black 96-well plate (Corning) and made up to 100 μl with a 1:1 (v/v) mixture of water and TNE buffer, before being stained with 100 μl of Hoechst solution (10 μg/ml Hoechst-33342 (Life Technologies) in a 1:1 mixture of water and TNE buffer). Fluorescence was measured at 360-nm excitation and 440-nm emission, using the Infinite M1000 Pro (Tecan). DNA content was quantified using a standard curve of salmon sperm DNA.

Western blotting

Following treatment, cells were washed three times with ice-cold PBS and lysed at room temperature in PBS supplemented with 1% (w/v) SDS, protease inhibitors (Roche Applied Science), and phosphatase inhibitors (64). Lysates were processed as described previously (65). Briefly, cells were scraped, sonicated (1 s on/off for 20 s total), and centrifuged at 16,000 $\times$ *g* for 20 min at 18 °C. After removal of the lipid layer, the protein content of the supernatant was quantified using the Pierce bicinchoninic acid assay kit (Thermo Fisher Scientific). Cell lysate (10 μg) was resolved by SDS-PAGE, transferred to polyvinylidene difluoride membranes (Millipore), and immunoblotted as described previously (55). Antibodies detecting pS473-Akt (clone 587F11, #4051), pT308-Akt (#9275), Akt (clone 11E7, #4685), and pT642-AS160 (#4288) were obtained from Cell Signaling Technology. The antibodies detecting PDH-E1α (clone H-131, #sc-292543) and 14-3-3 (clone K-19, #sc-629) were obtained from Santa Cruz Biotechnology, Inc. The antibody detecting pS293-PDH-E1α (#ABS204) was obtained from Millipore. Densitometric analysis was performed using either ImageJ software or LI-COR Image Studio.

Metabolic assays in primary adipocytes

Mature primary adipocytes were isolated from rats and subjected to metabolic assays, similarly in principle to previous studies (*e.g.* see Ref. 17), but with several modifications in buffer composition and miniaturization of assays into a multiwell format.

Isolation and assay buffers—Buffers included Krebs–Henseleit buffer (KHB: 120 mM NaCl, 4.7 mM KCl, 1.18 mM KH_2PO_4, 1.17 mM $MgSO_4$, 1.8 mM $CaCl_2$, 30 mM Na-HEPES, pH 7.4, 1 mM $NaHCO_3$ (added fresh), 1% (w/v) fatty acid–free BSA (Sigma), pH adjusted to 7.4 with NaOH), KHB-Glc buffer (KHB supplemented with 10 mM glucose), and assay buffer (HSF-DMEM supplemented with 1 mM $NaHCO_3$ (added fresh), 1 mM glutamine, 1 mM GlutaMAX, and 1% (w/v) fatty acid–free BSA, with pH adjusted to 7.4 with NaOH). All buffers were maintained at 37 °C throughout the experiment.

Isolation of mature primary adipocytes—Male Sprague–Dawley rats were housed at 23 °C in individually ventilated cages on a 12-h light/dark cycle with *ad libitum* access to standard rodent chow and water. Rat experiments were approved by the University of Sydney Animal Ethics Committee (project 2018/1418).

At 7–8 weeks of age (200–300 g), rats were sacrificed with CO_2. Epididymal fat pads were isolated in KHB-Glc buffer and minced before collagenase Type 1 (Worthington #CLS-1/LS004196) was added to achieve a final concentration of 0.5 mg/ml, with 3 ml of buffer volume per 1 g of tissue. Tissues were incubated with gentle rocking at 37 °C until digested (~45 min), tapped once to break apart digested tissue, and filtered through a 200-μm nylon mesh (SpectraMesh, VWR #SPEC146487) into conical tubes. The isolated adipocytes were resuspended in KHB and allowed to float to the top before the infranatant was removed. This wash step was repeated once with KHB and twice with assay buffer. These washes served to remove not only collagenase and nonadipocyte cells (66), but also glucose from the digestion buffer, as well as to condition the adipocytes to the assay buffer. After the final wash, the infranatant was removed, and 200-μl aliquots of adipocyte suspension were dispensed using cut pipette tips for various assays (Fig. 3*A*), described below. These assays were performed in parallel from the same batch of adipocytes, with each batch being sourced from 5–6 rats.

Collection of untreated primary adipocytes—Cells were dispensed into microcentrifuge tubes, which were immediately frozen in dry ice. These aliquots were used for DNA quantification (Fig. 3*A*, *Aliquot 1*) and served as a $t = 0$ control for glucose and lactate assays (Fig. 3*A*, *Aliquot 2*).

Stable tracer experiments in primary adipocytes—To assess glucose uptake and lactate production (Fig. 3*A*, *Aliquot 2*), cells were dispensed into 24-well polystyrene tissue culture microplates (Corning). To each well, 50 μl of prewarmed assay buffer containing [U-^{13}C]glucose, PBS, and/or insulin was added. As a result, each well contained a 250-μl final volume with 5 mM [U-^{13}C]glucose and either PBS control or 20 nM insulin. Plates were then immediately sealed with TopSeal-A PLUS (PerkinElmer Life Sciences) and gently rocked for 1 h with a rocking platform in a 37 °C incubator.

Following treatment, cells were quenched by freezing the plates on dry ice and stored at −80 °C until further processing. Plates were thawed, and lysate was resuspended in extraction buffer, which contained a 1:1 mixture of LC-grade MeOH and water, supplemented with 78.125 nM D-camphor-10-sulfonic acid (Wako #037-01032) as an internal standard. More specifically, to each well, 400 μl of extraction buffer was added, and lysate was scraped into the buffer and transferred to a microcentrifuge tube. The well was washed with another 400 μl of extraction buffer, such that the tube contained lysate resuspended with 800 μl of extraction buffer. To each tube, 800 μl of $CHCl_3$ was added, and then the mixture was briefly vortexed

and centrifuged for 20 min at 16,000 × *g* and 4 °C. The supernatant was lyophilized using an EZ-2 centrifugal evaporator (GeneVac), resuspended in 500 μl of water, and recentrifuged. The resulting supernatant was assessed for glucose uptake by enzymatic assay, and lactate production was assessed by LC-MS, both as described above. In both assays, calibration standards were added to $t = 0$ adipocyte samples, either before or after extraction, and assayed in parallel to the samples. Naive samples were generated by spiking the 5× mixture of [U-^{13}C]-glucose and PBS/insulin into the $t = 0$ adipocyte samples prior to extraction in parallel to the samples.

Radiotracer experiments in primary adipocytes—To assess glucose oxidation (Fig. 3*A*, *Aliquot 3*) or incorporation into lipid (Fig. 3*A*, *Aliquot 4*), cells were treated similarly as in the ^{13}C-tracer experiments above. Cells were dispensed into 24-well microplates and treated with 50 μl of prewarmed assay buffer containing glucose, [U-^{14}C]glucose, PBS, and/or insulin. As a result, each well contained a final volume of 250 μl, with 5 mM glucose and 1 μCi/ml [U-^{14}C]glucose, and either PBS control or 20 nM insulin. For the glucose oxidation assay, gas traps were also installed as described previously (56). Plates were then immediately sealed with TopSeal-A PLUS (PerkinElmer Life Sciences) and gently rocked for 1 h with a rocking platform in a 37 °C incubator.

Following treatment, glucose oxidation was measured as described above for cultured cells.

For incorporation into lipid, cells were quenched by freezing the plates on dry ice and stored at −80 °C until further processing. Plates were thawed, and lysate was transferred into polypropylene tubes by scraping lysates in 1 ml of 0.6% (w/v) NaCl (in water) followed by a wash with 100 μl of MeOH to collect residual debris. Lipids were extracted by MeOH/$CHCl_3$ extraction (67), with lysates resuspended in a final volume of 1 ml of 0.6% (w/v) NaCl and 4 ml of a 2:1 (v/v) mixture of $CHCl_3$/MeOH prior to extraction. An aliquot of the organic phase was evaporated to dryness under N_2 gas and resuspended in scintillant prior to assessing radiation as described for cultured cells; this determined the incorporation of glucose into the total lipid pool.

A second aliquot of the organic phase was evaporated to dryness and saponified using ethanolic KOH; dried lipids were resuspended in 1.5 ml of 1 M KOH and incubated at 70 °C for 15 min. 1 ml of EtOH was then added, and samples were vortexed before incubation at 70 °C for 2 h. Following saponification, lipids were acidified by the addition of 0.25 ml of 9 M H_2SO_4 (confirmed by pH litmus strips), and free lipids were isolated by three rounds of petroleum ether extraction (68). This involved mixing the saponified sample with 1 volume of petroleum ether (boiling point 60–80 °C) and incubating in dry ice to freeze the lower (aqueous) phase. The upper (organic) phase was then decanted into a separate tube, and the extraction was repeated twice more. The collected organic fraction (~7.5 ml) was then washed with 2.5 ml of water to remove any contaminating aqueous metabolites. The organic fraction was then evaporated to dryness under N_2 gas, and radioactivity was assayed as described above. This determined the incorporation of glucose into the saponifiable lipid pool. The difference between total and saponifiable lipid pools determined the incorporation of glucose into the nonsaponifiable lipid pool.

In all radiotracer experiments, cell-free controls included 1) naive media treated in parallel with the 5× mixture of glucose, radiotracer, and PBS/insulin and 2) undiluted extraction buffer (*e.g.* an aliquot of 0.6% (w/v) NaCl for the lipid incorporation assay). These were processed alongside the samples to account for any cell-independent background signal.

DNA quantification—The above metabolic measurements were normalized to cellular DNA content. DNA is typically isolated using proteinase K digestion and subsequent phenol/$CHCl_3$ extraction (69). However, the adipocytes were resuspended in a buffer containing 1% (w/v) BSA, rendering proteinase K digestion inefficient. As an alternative, DNA can be successfully isolated by freeze-thaw to promote cell lysis and exposure to high salt conditions (1 M NaCl) to disrupt DNA-protein interactions, which we employed for DNA normalization in cell culture experiments (described above). Organic extraction was also required to remove lipid, but we found that such high-salt conditions were incompatible with phenol/$CHCl_3$ extraction (data not shown), and subsequently used $CHCl_3$ alone for organic extraction.

Consequently, $t = 0$ adipocyte samples were thawed, and 500 μl of a 1:1 (v/v) mixture of water and TNE buffer was added. Samples were gently mixed before the addition of 500 μl of $CHCl_3$, mixing by inversion, and centrifugation for 20 min at 16,000 × *g* and 4 °C. The supernatant was collected and assayed directly for DNA content using SyBr stain (Life Technologies), according to the manufacturer's instructions. DNA content was quantified using a standard curve of salmon sperm DNA, added to naive assay buffer that had been extracted alongside the adipocyte samples. Extraction efficiency was determined by adding salmon sperm DNA to a subset of adipocyte samples, which were extracted and assayed in parallel to the samples.

Methodology for Drosophila experiments

Fly stocks, maintenance, and crosses—Fly strains used in this study included CG-none RNAi GD12145 (Vienna Drosophila Resource Center) and *Ldh* RNAi GD6887 (#31192, Vienna Drosophila Resource Center), *ubiquitous*-GAL4/Cyo (Bloomington #32551), and *CG*-Gal4 (Bloomington #7011).

Flies were maintained at standard temperature, humidity, and 12-h light/dark cycle. Flies were kept on a diet of 1% (w/v) agar (Sigma-Aldrich #A1296), 10% (w/v) brewer's yeast (MP Biomedicals #290331225), and 5% (w/v) sugar (Coles, Hawthorne East, Australia), supplemented with 3% (w/v) methyl 4-hydroxybenzoate (Sigma-Aldrich #H3647) and 0.3% (v/v) propionic acid (Sigma-Aldrich #P5561) as preservatives.

To generate fat body–specific knockdown of *Ldh* (or corresponding control), 20 CG-Gal4 females were crossed with five *Ldh* RNAi or CG-none male flies, respectively. For whole-body knockdown of *Ldh* (or corresponding control), *ubiquitous*-GAL4/Cyo females were used instead.

Fly glucose tolerance test—The fly glucose tolerance test was performed similarly in principle to previous studies (70), but modified to enhance assay sensitivity, including a shorter "feed" phase, additional time points, and organic extraction to preserve metabolite stability.

For each biological replicate, 15 adult (3–5-day-old) male flies were collected and starved for 16 h in a vial with a Kimwipe that was soaked with 1 ml of water. During the feed phase of the assay, flies were transferred to vials with Kimwipes, each soaked in 1 ml of 10% (w/v) D-glucose (Sigma). After 30 min, flies underwent the "post-feed" phase of the assay, being starved again for up to 60 min. Every 15 min throughout the assay, from just prior to the feed phase ($t = 0$ min) to the end of the post-feed phase, six vials (biological replicates) were harvested for each genotype.

Flies were initially quenched by emptying the vial into a small sieve (derived from a tea strainer) in isopropyl alcohol. The sieve was transferred to increasingly diluted solutions of isopropyl alcohol (50, 25, 10, 5, and 0% (v/v) diluted with water) to wash flies of any uneaten food. Flies were then subjected to MeOH/$CHCl_3$ extraction (67): flies were transferred to a round-bottom microcentrifuge tube, 200 μl of a 2:1 (v/v) mixture of $CHCl_3$/MeOH was added, and flies were homogenized with a 5-mm steel bead (Qiagen #69989) for 30 s at 30 Hz (Mixer Mill MM 400, Retsch). 600 μl of $CHCl_3$/MeOH mixture was added, followed by 200 μl of 0.6% (w/v) NaCl in water, and samples were briefly vortexed before being centrifuged for 20 min at 16,000 $\times$ *g* and 4 °C. The supernatant was lyophilized using an EZ-2 centrifugal evaporator (GeneVac), resuspended in water, and recentrifuged briefly to clear debris. Glucose and lactate content were determined enzymatically as described above.

Fly food intake assay—This assay relied on the principle that when blue food dye is added to fly food, the amount of ingested dye can serve as a proxy for food intake during short-term experiments (28). Flies were treated similarly to the glucose tolerance test, with a 16-h fast and a 30-min feed phase, except during the feed phase, vials contained Kimwipes soaked with 10% (w/v) glucose and 0.05% (v/v) FD&C1 blue dye (Queenie Brand, Coles). At the end of the feed phase, flies were washed in isopropyl alcohol and homogenized as in the glucose tolerance test, except homogenization was performed in 100 μl of water. Samples were briefly centrifuged to clear debris, and the supernatant was lyophilized using an EZ-2 centrifugal evaporator. Samples were reconstituted in 50 μl of water, and absorbance at 628 nm was measured. Blue dye content was quantified by comparison with a standard curve of blue dye.

Fly radiotracer experiments—To measure glucose incorporation into CO_2, lipid, and glycogen, experiments were performed as described previously (56). Briefly, for each biological replicate, 10 male adult (3–5-day-old) flies were starved for 16 h as described for the glucose tolerance test. Flies were transferred to a well in a 12-well tissue culture plate, which contained food with [U-^{14}C]glucose radiotracer (1% (w/v) agar, 5% (w/v) D-glucose, 10% (w/v) bakers' yeast, 0.5 μCi/ml [U-^{14}C]glucose, 0.05% (v/v) FD&C1 food coloring). Gas traps were installed, and plates were sealed for 3 h, after which trapped CO_2 was measured by liquid scintillation counting to assess glucose oxidation. Plates were then resealed and frozen at −80 °C to quench the flies.

To assess glucose incorporation into glycogen or lipid, plates were thawed and flies were washed in isopropyl alcohol and homogenized as described for the glucose tolerance test. For glycogen, homogenization was performed in 200 μl of 1 M KOH, after which glycogen was isolated by Na_2SO_4 precipitation and radioactivity was measured by liquid scintillation counting, as described above. For lipid, homogenization was performed in 200 μl of 0.6% (w/v) NaCl, after which lipid was isolated by MeOH/$CHCl_3$ extraction as described in the primary adipocyte radiotracer experiments, except adjusted to a smaller sample volume. An aliquot of isolated lipid was assessed for radioactivity by liquid scintillation counting, and a second aliquot was saponified and radioactivity was assessed, as described for the primary adipocyte radiotracer experiments.

RNA isolation and quantitative PCR of knockdown—For each biological replicate, 10 adult male flies were homogenized with a 5-mm steel bead (Qiagen #69989) for 30 s at 30 Hz (Mixer Mill MM 400, Retsch), in 200 μl of TRIzol reagent (Invitrogen). RNA was extracted with 1,3-bromochloropopane and precipitated with isopropyl alcohol as described previously (71). RNA quality and quantity were assessed by a Nanodrop 2000c (Thermo Scientific), and reverse-transcribed using PrimeScript (TakaraBio), according to the manufacturer's instructions. RNA expression was measured by quantitative real-time PCR, using Fast-Start SyBr Mix (Roche Applied Science) and a Lightcycler 480 II (Roche Applied Science), according to the manufacturer's instructions. Primers were used to amplify the following genes: *Ldh* (forward, 5′-CTCAAGAACATCATCCCCAAGC-3′; reverse, 5′-TTCCAGGCCACGTAGGTCA-3′), *tubulin* (forward, 5′-TGTCGCGTGTGAAACACTTC-3′; reverse, 5′-AGCAGGCGTTTCCAATCTG-3′). PCR efficiency was confirmed in each run by a serial dilution of pooled sample. Gene expression was calculated using the $\Delta\Delta C_t$ method.

Author contributions—J. R. K., G. J. C., and D. E. J. conceptualization; J. R. K. and L.-E. Q. formal analysis; J. R. K., D. F., G. J. C., and D. E. J. funding acquisition; J. R. K., L.-E. Q., D. F., D. J. F., S. D. E., A. D.-V., K. C. C., F. C. W., X. D., A. H., S. I., and Y. K. investigation; J. R. K., L.-E. Q., D. F., S. K., G. J. C., and D. E. J. methodology; J. R. K., D. J. F., G. J. C., and D. E. J. writing-original draft; J. R. K., L.-E. Q., D. F., D. J. F., S. D. E., A. D.-V., K. C. C., F. C. W., X. D., S. K., P.-X. Z., U. K. T., A. H., S. I., Y. K., T. S., G. J. C., and D. E. J. writing-review and editing; P.-X. Z. and U. K. T. resources; T. S., G. J. C., and D. E. J. supervision.

Acknowledgments—We thank the Charles Perkins Centre (CPC) Research Support team, particularly Dr. Ian Garthwaite, Dr. Natalia Magarinos, Harry Simpson, Dr. Melissa Gardiner, and Dr. Macarena Rodriguez, for technical support. We also thank Dr. John O'Sullivan, Dr. Sigrid Jall, and Dr. Marin Nelson for technical advice. This research was facilitated by access to Sydney Mass Spectrometry, a core research facility at the University of Sydney.

References

1. Rosen, E. D., and Spiegelman, B. M. (2014) What we talk about when we talk about fat. *Cell* **156,** 20–44 CrossRef Medline
2. Garvey, W. T., and Kolterman, O. G. (1988) Correlation of *in vivo* and *in vitro* actions of insulin in obesity and noninsulin-dependent diabetes mellitus: role of the glucose transport system. *Diabetes Metab Rev.* **4,** 543–569 CrossRef Medline
3. Kraegen, E. W., Clark, P. W., Jenkins, A. B., Daley, E. A., Chisholm, D. J., and Storlien, L. H. (1991) Development of muscle insulin resistance after liver insulin resistance in high-fat-fed rats. *Diabetes* **40,** 1397–1403 CrossRef Medline

4. Turner, N., Kowalski, G. M., Leslie, S. J., Risis, S., Yang, C., Lee-Young, R. S., Babb, J. R., Meikle, P. J., Lancaster, G. I., Henstridge, D. C., White, P. J., Kraegen, E. W., Marette, A., Cooney, G. J., Febbraio, M. A., and Bruce, C. R. (2013) Distinct patterns of tissue-specific lipid accumulation during the induction of insulin resistance in mice by high-fat feeding. *Diabetologia* **56,** 1638–1648 CrossRef Medline
5. DeFronzo, R. A., and Tripathy, D. (2009) Skeletal muscle insulin resistance is the primary defect in type 2 diabetes. *Diabetes Care* **32,** S157–S163 CrossRef Medline
6. Abel, E. D., Peroni, O., Kim, J. K., Kim, Y. B., Boss, O., Hadro, E., Minnemann, T., Shulman, G. I., and Kahn, B. B. (2001) Adipose-selective targeting of the GLUT4 gene impairs insulin action in muscle and liver. *Nature* **409,** 729–733 CrossRef Medline
7. Herman, M. A., Peroni, O. D., Villoria, J., Schön, M. R., Abumrad, N. A., Blüher, M., Klein, S., and Kahn, B. B. (2012) A novel ChREBP isoform in adipose tissue regulates systemic glucose metabolism. *Nature* **484,** 333–338 CrossRef Medline
8. Vander Heiden, M. G., Cantley, L. C., and Thompson, C. B. (2009) Understanding the Warburg effect: the metabolic requirements of cell proliferation. *Science* **324,** 1029–1033 CrossRef Medline
9. DiGirolamo, M., Newby, F. D., and Lovejoy, J. (1992) Lactate production in adipose tissue: a regulated function with extra-adipose implications. *FASEB J.* **6,** 2405–2412 CrossRef Medline
10. Tanner, L. B., Goglia, A. G., Wei, M. H., Sehgal, T., Parsons, L. R., Park, J. O., White, E., Toettcher, J. E., and Rabinowitz, J. D. (2018) Four key steps control glycolytic flux in mammalian cells. *Cell Syst.* **7,** 49–62.e8 CrossRef Medline
11. Hui, S., Ghergurovich, J. M., Morscher, R. J., Jang, C., Teng, X., Lu, W., Esparza, L. A., Reya, T., Zhan, L., Yanxiang Guo, J., White, E., and Rabinowitz, J. D. (2017) Glucose feeds the TCA cycle via circulating lactate. *Nature* **551,** 115–118 CrossRef Medline
12. Cori, C. F., and Cori, G. T. (1929) Glycogen formation in the liver from D- and L-lactic acid. *J. Biol. Chem.* **81,** 389–403
13. Sabater, D., Arriarán, S., Romero Mdel, M., Agnelli, S., Remesar, X., Fernández-López, J. A., and Alemany, M. (2014) Cultured 3T3L1 adipocytes dispose of excess medium glucose as lactate under abundant oxygen availability. *Sci. Rep.* **4,** 3663 CrossRef Medline
14. Palfreyman, R. W., Clark, A. E., Denton, R. M., Holman, G. D., and Kozka, I. J. (1992) Kinetic resolution of the separate GLUT1 and GLUT4 glucose transport activities in 3T3-L1 cells. *Biochem. J.* **284,** 275–282 CrossRef Medline
15. Krycer, J. R., Fisher-Wellman, K. H., Fazakerley, D. J., Muoio, D. M., and James, D. E. (2017) Bicarbonate alters cellular responses in respiration assays. *Biochem. Biophys. Res. Commun.* **489,** 399–403 CrossRef Medline
16. Krycer, J. R., Yugi, K., Hirayama, A., Fazakerley, D. J., Quek, L. E., Scalzo, R., Ohno, S., Hodson, M. P., Ikeda, S., Shoji, F., Suzuki, K., Domanova, W., Parker, B. L., Nelson, M. E., Humphrey, S. J., Turner, N., Hoehn, K. L., Cooney, G. J., Soga, T., Kuroda, S., and James, D. E. (2017) Dynamic metabolomics reveals that insulin primes the adipocyte for glucose metabolism. *Cell Rep.* **21,** 3536–3547 CrossRef Medline
17. Crandall, D. L., Fried, S. K., Francendese, A. A., Nickel, M., and DiGirolamo, M. (1983) Lactate release from isolated rat adipocytes: influence of cell size, glucose concentration, insulin and epinephrine. *Horm. Metab. Res.* **15,** 326–329 CrossRef Medline
18. Fazakerley, D. J., Chaudhuri, R., Yang, P., Maghzal, G. J., Thomas, K. C., Krycer, J. R., Humphrey, S. J., Parker, B. L., Fisher-Wellman, K. H., Meoli, C. C., Hoffman, N. J., Diskin, C., Burchfield, J. G., Cowley, M. J., Kaplan, W., *et al.* (2018) Mitochondrial CoQ deficiency is a common driver of mitochondrial oxidants and insulin resistance. *Elife* **7,** e32111 CrossRef Medline
19. Hoehn, K. L., Salmon, A. B., Hohnen-Behrens, C., Turner, N., Hoy, A. J., Maghzal, G. J., Stocker, R., Van Remmen, H., Kraegen, E. W., Cooney, G. J., Richardson, A. R., and James, D. E. (2009) Insulin resistance is a cellular antioxidant defense mechanism. *Proc. Natl. Acad. Sci. U.S.A.* **106,** 17787–17792 CrossRef Medline
20. Tso, S. C., Qi, X., Gui, W. J., Wu, C. Y., Chuang, J. L., Wernstedt-Asterholm, I., Morlock, L. K., Owens, K. R., Scherer, P. E., Williams, N. S., Tambar, U. K., Wynn, R. M., and Chuang, D. T. (2014) Structure-guided development of specific pyruvate dehydrogenase kinase inhibitors targeting the ATP-binding pocket. *J. Biol. Chem.* **289,** 4432–4443 CrossRef Medline
21. Boudreau, A., Purkey, H. E., Hitz, A., Robarge, K., Peterson, D., Labadie, S., Kwong, M., Hong, R., Gao, M., Del Nagro, C., Pusapati, R., Ma, S., Salphati, L., Pang, J., Zhou, A., *et al.* (2016) Metabolic plasticity underpins innate and acquired resistance to LDHA inhibition. *Nat. Chem. Biol.* **12,** 779–786 CrossRef Medline
22. Holmes, W. F. (1959) Locating sites of interactions between external chemicals and a sequence of chemical reactions. *Trans. Faraday Soc.* **55,** 1122–1126 CrossRef
23. Moreno-Sánchez, R., Saavedra, E., Rodríguez-Enríquez, S., and Olín-Sandoval, V. (2008) Metabolic control analysis: a tool for designing strategies to manipulate metabolic pathways. *J. Biomed. Biotechnol.* **2008,** 597913 CrossRef Medline
24. Billiard, J., Dennison, J. B., Briand, J., Annan, R. S., Chai, D., Colón, M., Dodson, C. S., Gilbert, S. A., Greshock, J., Jing, J., Lu, H., McSurdy-Freed, J. E., Orband-Miller, L. A., Mills, G. B., Quinn, C. J., *et al.* (2013) Quinoline 3-sulfonamides inhibit lactate dehydrogenase A and reverse aerobic glycolysis in cancer cells. *Cancer Metab.* **1,** 19 CrossRef Medline
25. Le, A., Cooper, C. R., Gouw, A. M., Dinavahi, R., Maitra, A., Deck, L. M., Royer, R. E., Vander Jagt, D. L., Semenza, G. L., and Dang, C. V. (2010) Inhibition of lactate dehydrogenase A induces oxidative stress and inhibits tumor progression. *Proc. Natl. Acad. Sci. U.S.A.* **107,** 2037–2042 CrossRef Medline
26. Wyatt, G. R., and Kale, G. F. (1957) The chemistry of insect hemolymph. II. Trehalose and other carbohydrates. *J. Gen. Physiol.* **40,** 833–847 CrossRef Medline
27. Elbein, A. D., Pan, Y. T., Pastuszak, I., and Carroll, D. (2003) New insights on trehalose: a multifunctional molecule. *Glycobiology* **13,** 17R–27R CrossRef Medline
28. Shell, B. C., Schmitt, R. E., Lee, K. M., Johnson, J. C., Chung, B. Y., Pletcher, S. D., and Grotewiel, M. (2018) Measurement of solid food intake in *Drosophila* via consumption-excretion of a dye tracer. *Sci. Rep.* **8,** 11536 CrossRef Medline
29. Francis, D., Krycer, J. R., Cooney, G. J., and James, D. E. (2019) A modified gas-trapping method for high-throughput metabolic experiments in *Drosophila melanogaster*. *BioTechniques* **67,** 123–125 CrossRef Medline
30. Cantor, J. R., Abu-Remaileh, M., Kanarek, N., Freinkman, E., Gao, X., Louissaint, A., Jr., Lewis, C. A., and Sabatini, D. M. (2017) Physiologic medium rewires cellular metabolism and reveals uric acid as an endogenous inhibitor of UMP synthase. *Cell* **169,** 258–272.e17 CrossRef Medline
31. Digirolamo, M., Thacker, S. V., and Fried, S. K. (1993) Effects of cell density on *in vitro* glucose metabolism by isolated adipocytes. *Am. J. Physiol.* **264,** E361–E366 CrossRef Medline
32. Kashiwagi, A., Verso, M. A., Andrews, J., Vasquez, B., Reaven, G., and Foley, J. E. (1983) *In vitro* insulin resistance of human adipocytes isolated from subjects with noninsulin-dependent diabetes mellitus. *J. Clin. Invest.* **72,** 1246–1254 CrossRef Medline
33. Mårin, P., Rebuffé-Scrive, M., Smith, U., and Björntorp, P. (1987) Glucose uptake in human adipose tissue. *Metabolism* **36,** 1154–1160 CrossRef Medline
34. Thacker, S. V., Nickel, M., and DiGirolamo, M. (1987) Effects of food restriction on lactate production from glucose by rat adipocytes. *Am. J. Physiol.* **253,** E336–E342 CrossRef Medline
35. Newby, F. D., Sykes, M. N., and DiGirolamo, M. (1988) Regional differences in adipocyte lactate production from glucose. *Am. J. Physiol.* **255,** E716–E722 CrossRef Medline
36. Newby, F. D., Wilson, L. K., Thacker, S. V., and DiGirolamo, M. (1990) Adipocyte lactate production remains elevated during refeeding after fasting. *Am. J. Physiol.* **259,** E865–E871 CrossRef Medline
37. Bernstein, R. S., Zimmerman, K. S., and Carney, A. L. (1981) Absence of impaired glucose utilization in adipocytes from rats fed a carbohydrate-free, high protein diet. *J. Nutr.* **111,** 237–243 CrossRef Medline
38. Newby, F. D., Bayo, F., Thacker, S. V., Sykes, M., and DiGirolamo, M. (1989) Effects of streptozocin-induced diabetes on glucose metabolism and lactate release by isolated fat cells from young lean and older, moderately obese rats. *Diabetes* **38,** 237–243 CrossRef Medline

39. Lovejoy, J., Newby, F. D., Gebhart, S. S., and DiGirolamo, M. (1992) Insulin resistance in obesity is associated with elevated basal lactate levels and diminished lactate appearance following intravenous glucose and insulin. *Metabolism* **41,** 22–27 CrossRef Medline
40. Lovejoy, J., Mellen, B., and Digirolamo, M. (1990) Lactate generation following glucose ingestion: relation to obesity, carbohydrate tolerance and insulin sensitivity. *Int. J. Obes.* **14,** 843–855 Medline
41. Walz, W., and Mukerji, S. (1988) Lactate production and release in cultured astrocytes. *Neurosci. Lett.* **86,** 296–300 CrossRef Medline
42. Dringen, R., Gebhardt, R., and Hamprecht, B. (1993) Glycogen in astrocytes: possible function as lactate supply for neighboring cells. *Brain Res.* **623,** 208–214 CrossRef Medline
43. Shipp, J. C., Opie, L. H., and Challoner, D. (1961) Fatty acid and glucose metabolism in the perfused heart. *Nature* **189,** 1018–1019 CrossRef
44. Consoli, A., Nurjhan, N., Reilly, J. J., Jr., Bier, D. M., and Gerich, J. E. (1990) Contribution of liver and skeletal muscle to alanine and lactate metabolism in humans. *Am. J. Physiol.* **259,** E677–E684 CrossRef Medline
45. Kerckhoffs, D. A., Arner, P., and Bolinder, J. (1998) Lipolysis and lactate production in human skeletal muscle and adipose tissue following glucose ingestion. *Clin. Sci.* (*Lond.*) **94,** 71–77 CrossRef Medline
46. Frayn, K. N., Coppack, S. W., Humphreys, S. M., and Whyte, P. L. (1989) Metabolic characteristics of human adipose tissue *in vivo*. *Clin. Sci.* (*Lond.*) **76,** 509–516 CrossRef Medline
47. Yki-Järvinen, H., Bogardus, C., and Foley, J. E. (1990) Regulation of plasma lactate concentration in resting human subjects. *Metabolism* **39,** 859–864 CrossRef Medline
48. Frayn, K. N., and Humphreys, S. M. (2012) Metabolic characteristics of human subcutaneous abdominal adipose tissue after overnight fast. *Am. J. Physiol. Endocrinol. Metab.* **302,** E468–E475 CrossRef Medline
49. Hodson, L., Humphreys, S. M., Karpe, F., and Frayn, K. N. (2013) Metabolic signatures of human adipose tissue hypoxia in obesity. *Diabetes* **62,** 1417–1425 CrossRef Medline
50. Hagström, E., Arner, P., Ungerstedt, U., and Bolinder, J. (1990) Subcutaneous adipose tissue: a source of lactate production after glucose ingestion in humans. *Am. J. Physiol.* **258,** E888–E893 CrossRef Medline
51. Jansson, P. A., Larsson, A., Smith, U., and Lönnroth, P. (1994) Lactate release from the subcutaneous tissue in lean and obese men. *J. Clin. Invest.* **93,** 240–246 CrossRef Medline
52. Pearce, F. J., and Connett, R. J. (1980) Effect of lactate and palmitate on substrate utilization of isolated rat soleus. *Am. J. Physiol.* **238,** C149–C159 CrossRef Medline
53. Landau, B. R., and Wahren, J. (1988) Quantification of the pathways followed in hepatic glycogen formation from glucose. *FASEB J.* **2,** 2368–2375 CrossRef Medline
54. Ahmed, K., Tunaru, S., Tang, C., Müller, M., Gille, A., Sassmann, A., Hanson, J., and Offermanns, S. (2010) An autocrine lactate loop mediates insulin-dependent inhibition of lipolysis through GPR81. *Cell Metab.* **11,** 311–319 CrossRef Medline
55. Fazakerley, D. J., Naghiloo, S., Chaudhuri, R., Koumanov, F., Burchfield, J. G., Thomas, K. C., Krycer, J. R., Prior, M. J., Parker, B. L., Murrow, B. A., Stöckli, J., Meoli, C. C., Holman, G. D., and James, D. E. (2015) Proteomic analysis of GLUT4 storage vesicles reveals tumor suppressor candidate 5 (TUSC5) as a novel regulator of insulin action in adipocytes. *J. Biol. Chem.* **290,** 23528–23542 CrossRef Medline
56. Krycer, J. R., Diskin, C., Nelson, M. E., Zeng, X. Y., Fazakerley, D. J., and James, D. E. (2018) A gas trapping method for high-throughput metabolic experiments. *BioTechniques* **64,** 27–29 CrossRef Medline
57. Prabhu, A. V., Krycer, J. R., and Brown, A. J. (2013) Overexpression of a key regulator of lipid homeostasis, Scap, promotes respiration in prostate cancer cells. *FEBS Lett.* **587,** 983–988 CrossRef Medline
58. Van Handel, E. (1965) Estimation of glycogen in small amounts of tissue. *Anal. Biochem.* **11,** 256–265 CrossRef Medline
59. Thompson, A. L., Lim-Fraser, M. Y., Kraegen, E. W., and Cooney, G. J. (2000) Effects of individual fatty acids on glucose uptake and glycogen synthesis in soleus muscle *in vitro*. *Am. J. Physiol. Endocrinol. Metab.* **279,** E577–E584 CrossRef Medline
60. Lu, W., Clasquin, M. F., Melamud, E., Amador-Noguez, D., Caudy, A. A., and Rabinowitz, J. D. (2010) Metabolomic analysis via reversed-phase ion-pairing liquid chromatography coupled to a stand alone orbitrap mass spectrometer. *Anal. Chem.* **82,** 3212–3221 CrossRef Medline
61. Zhang, W., Guo, C., Jiang, K., Ying, M., and Hu, X. (2017) Quantification of lactate from various metabolic pathways and quantification issues of lactate isotopologues and isotopmers. *Sci. Rep.* **7,** 8489 CrossRef Medline
62. Buescher, J. M., Antoniewicz, M. R., Boros, L. G., Burgess, S. C., Brunengraber, H., Clish, C. B., DeBerardinis, R. J., Feron, O., Frezza, C., Ghesquiere, B., Gottlieb, E., Hiller, K., Jones, R. G., Kamphorst, J. J., Kibbey, R. G., *et al.* (2015) A roadmap for interpreting ^{13}C metabolite labeling patterns from cells. *Curr. Opin. Biotechnol.* **34,** 189–201 CrossRef Medline
63. Krycer, J. R., Phan, L., and Brown, A. J. (2012) A key regulator of cholesterol homoeostasis, SREBP-2, can be targeted in prostate cancer cells with natural products. *Biochem. J.* **446,** 191–201 CrossRef Medline
64. Kleinert, M., Parker, B. L., Chaudhuri, R., Fazakerley, D. J., Serup, A., Thomas, K. C., Krycer, J. R., Sylow, L., Fritzen, A. M., Hoffman, N. J., Jeppesen, J., Schjerling, P., Ruegg, M. A., Kiens, B., James, D. E., and Richter, E. A. (2016) mTORC2 and AMPK differentially regulate muscle triglyceride content via Perilipin 3. *Mol. Metab.* **5,** 646–655 CrossRef Medline
65. Krycer, J. R., Fazakerley, D. J., Cater, R. J., C. Thomas, K., Naghiloo, S., Burchfield, J. G., Humphrey, S. J., Vandenberg, R. J., Ryan, R. M., and James, D. E. (2017) The amino acid transporter, SLC1A3, is plasma membrane-localised in adipocytes and its activity is insensitive to insulin. *FEBS Lett.* **591,** 322–330 CrossRef Medline
66. Rodbell, M. (1964) Metabolism of isolated fat cells. I. Effects of hormones on glucose metabolism and lipolysis. *J. Biol. Chem.* **239,** 375–380 Medline
67. Folch, J., Lees, M., and Sloane Stanley, G. H. (1957) A simple method for the isolation and purification of total lipides from animal tissues. *J. Biol. Chem.* **226,** 497–509 Medline
68. Stansbie, D., Brownsey, R. W., Crettaz, M., and Denton, R. M. (1976) Acute effects *in vivo* of anti-insulin serum on rates of fatty acid synthesis and activities of acetyl-coenzyme A carboxylase and pyruvate dehydrogenase in liver and epididymal adipose tissue of fed rats. *Biochem. J.* **160,** 413–416 CrossRef Medline
69. Strauss, W. M. (2001) Preparation of genomic DNA from mammalian tissue. *Curr. Protoc. Mol. Biol.* Chapter 2, Unit 2.2 CrossRef Medline
70. Haselton, A., Sharmin, E., Schrader, J., Sah, M., Poon, P., and Fridell, Y. W. (2010) Partial ablation of adult *Drosophila* insulin-producing neurons modulates glucose homeostasis and extends life span without insulin resistance. *Cell Cycle* **9,** 3063–3071 CrossRef Medline
71. Krycer, J. R., and Brown, A. J. (2011) Cross-talk between the androgen receptor and the liver X receptor: implications for cholesterol homeostasis. *J. Biol. Chem.* **286,** 20637–20647 CrossRef Medline